Development of a yeast-based screening assay for inhibitors of the kinase chaperone Cdc37

José Pedro Ramos Guimarães
Mestrado em Bioquímica
Yeast Signalling Networks, i3S-Instituto de Investigação e Inovação em Saúde, Universidade do Porto
2022

Supervisor
Clara Isabel Ferreira Pereira, Professora Auxiliar, Instituto de Ciências Biomédicas Abel Salazar; Investigadora, IBMC/i3S, Universidade do Porto

Co-supervisor
Vitor Manuel Vieira da Costa, Professor Associado, Instituto de Ciências Biomédicas Abel Salazar, Investigador Principal, IBMC/i3S, Universidade do Porto


INSTITUTO DE INVESTIGAÇÃO
E INOVAÇÃO EM SAÚDE
UNIVERSIDADE DO PORTO


U.PORTO
ICBAS | INSTITUTO DE CIÊNCIAS BIOMÉDICAS ABEL SALAZAR
SCHOOL OF MEDICINE AND
BIOMEDICAL SCIENCES


U.PORTO
FACULDADE DE CIÊNCIAS
UNIVERSIDADE DO PORTO

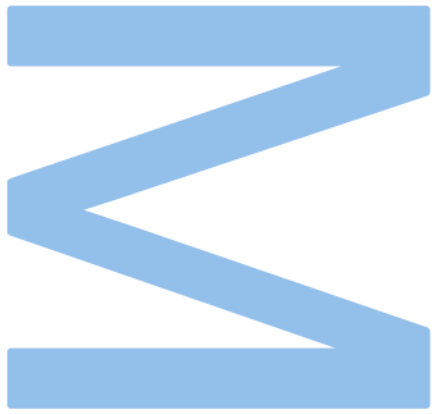

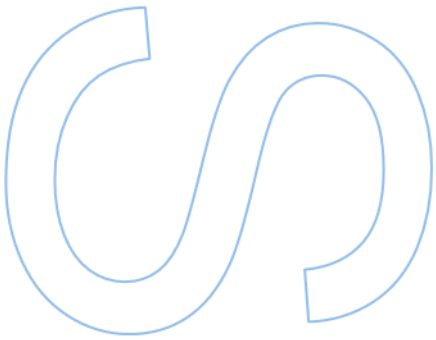

Sworn Statement

I, José Pedro Ramos Guimarães, enrolled in the Master Degree in Biochemistry at the Faculty of Sciences of the University of Porto hereby declare, in accordance with the provisions of paragraph a) of Article 14 of the Code of Ethical Conduct of the University of Porto, that the content of this dissertation reflects perspectives, research work and my own interpretations at the time of its submission.

By submitting this dissertation, I also declare that it contains the results of my own research work and contributions that have not been previously submitted to this or any other institution.

I further declare that all references to other authors fully comply with the rules of attribution and are referenced in the text by citation and identified in the bibliographic references section. This dissertation does not include any content whose reproduction is protected by copyright laws.

I am aware that the practice of plagiarism and self-plagiarism constitute a form of academic offense.

30-09-2022, Porto

Agradecimentos

Em primeiro lugar quero dirigir um enorme agradecimento à minha orientadora Clara Pereira que me recebeu e me guiou durante as várias etapas do desenvolvimento deste projeto. Não posso deixar de frisar o quão valiosas e enriquecedoras foram todas as lições que pacientemente me deste ao longo deste ano. Estiveste sempre disponível para esclarecer qualquer dúvida que tive e para me ajudar, quer seja na aprendizagem das diferentes técnicas laboratoriais que realizei, como na escrita da dissertação. Obrigado por confiares em mim para o desenvolvimento deste projeto, foi uma experiência que certamente nunca irei esquecer.

Queria também agradecer ao professor Vítor Costa pela oportunidade de realizar a minha dissertação de mestrado no grupo Yeast Signalling Networks e me auxiliar no decorrer do trabalho como coorientador. Agradeço também aos restantes elementos do grupo- Cláudia Leite, Telma Martins e Vítor Teixeira-, não só pela constante disponibilidade para o esclarecimento de dúvidas e auxiliar no trabalho, mas também por proporcionarem diariamente um ambiente acolhedor desde o início até ao fim desta jornada. À minha colega de mestrado e grupo, Eduarda Pinto, quero também deixar não só um agradecimento, mas também congratulá-la por mais um objetivo cumprido na conclusão do mestrado. Um agradecimento também aos investigadores da faculdade de farmácia da Universidade do Porto (FFUP) e do Centro Interdisciplinar de Investigação Marinha e Ambiental (CIIMAR) pelo fornecimento dos compostos usados, sem os quais este projeto não teria sido possível.

Tenho também de agradecer aos meus pais por toda a compreensão, amor e esforço investido em mim não só durante esta etapa, mas também durante toda a minha vida. Obrigado por acreditarem sempre em mim, por me fazerem feliz e por me inspirarem a nunca desistir nem deixar de acreditar em mim mesmo. Por fim queria dedicar à minha namorada, Ana Vilarinho, um agradecimento especial. Obrigado por me acompanhares e partilhares comigo mais esta etapa da minha vida neste planeta suportado por quatro elefantes carregados no topo da carapaça de uma grande e nobre tartaruga. Que a próxima etapa das nossas vidas seja tão interessante como esta.

Resumo

Em eucariontes, várias proteínas requerem chaperonas moleculares para a aquisição da conformação correta. A proteína de choque térmico 90 (Hsp90) é uma proteína chaperona altamente conservada e ubiquamente expressa. A Hsp90 forma complexos com outras proteínas, chamadas co-chaperonas, responsáveis pela aquisição de especificidade. A proteína ciclo de divisão celular 37 (Cdc37) é a co-chaperona que permite que a Hsp90 interaja especificamente com quinases. A disfunção do complexo chaperona constituído pelas proteínas Hsp90 e Cdc37 está associada com o desenvolvimento de doenças neurodegenerativas assim como com o desenvolvimento de cancro através da dependência oncogénica e perpetuação da sobrevivência de células cancerígenas. Dada a correlação entre Hsp90/complexo Hsp90-Cdc37 e doença, a identificação de inibidores que têm como alvo este complexo é de elevada importância.

Neste trabalho, tivemos como objetivo implementar um modelo de pesquisa em levedura para identificar inibidores do complexo Hsp90-Cdc37. *Saccharomyces cerevisiae,* um eucarionte unicelular simples, ocupa uma posição privilegiada no que diz respeito à pesquisa de compostos nas etapas iniciais da descoberta de fármacos. Neste trabalho, tiramos proveito de um mutante que expressa uma forma mutada da quinase Cdc28 (*cdc28-1*), que ao possuir uma dependência aumentada no sistema Hsp90-Cdc37, funciona como um indicador da atividade deste complexo. Usando uma estirpe parental hipersensível a drogas, foi-nos possível implementar ensaios simples de halos de inibição para a pesquisa de compostos. Confirmamos que a mutação *cdc28-1* exibe maior sensibilidade do que células parentais para inibidores estabelecidos da Hsp90 (GDA e 17-AAG) mas não para antifúngicos gerais. Usando este modelo, pesquisamos uma biblioteca de compostos e identificamos seis xantonas como potenciais inibidores do complexo Hsp90-Cdc37. A inibição da Hsp90 por duas destas xantonas também foi confirmada através da avaliação da depleção dos níveis de Cdc28. Futuramente, será ainda necessário determinar o mecanismo de ação dos compostos, nomeadamente, identificar se estes são disruptores da interação formada pelo complexo Hsp90-Cdc37 ou se são inibidores diretos das proteínas Hsp90 ou Cdc37. Estes compostos poderão ser usados no desenvolvimento de novas moléculas com maior potência e seletividade para potencial uso terapêutico.

Palavras-Chave

Enrolamento proteico, Chaperona molecular, Modelo de pesquisa em levedura, Inibição de Hsp90, Inibição de Hsp90-Cdc37

Abstract

In eukaryotes many proteins require molecular chaperones to acquire proper folding. Heat shock protein 90 (Hsp90) is a highly conserved and ubiquitously expressed protein chaperone that establishes complexes with other proteins called co-chaperones to achieve selectivity. Cell division cycle 37 (Cdc37) is a co-chaperone that allows Hsp90 to interact specifically with kinases. Malfunction of the Hsp90-Cdc37 chaperone complex has been associated with the development of neurodegenerative diseases as well the development of cancer through oncogene addiction and cancer survival. Given the correlation between Hsp90/Hsp90-Cdc37 chaperone complex and disease, the identification of inhibitors that target this complex is of major importance.

In this work we aimed to implement a yeast screening model for Hsp90-Cdc37 inhibitors. *Saccharomyces cerevisiae*, a simple unicellular eukaryote, occupies a privileged position in compound screening in the early stages of drug discovery. We took advantage of the higher dependency on the Hsp90-Cdc37 system of a kinase Cdc28 mutant version (*cdc28-1*) as a readout for chaperone activity. Using a drug hypersensitive strain as parental strain, we were able to implement simple halo assays for compound screening. We confirmed that *cdc28-1* mutations are more sensitive than wild-type cells to well-established Hsp90 inhibitors (GDA and 17-AAG) but not to unrelated antifungals. Using this model, we screened a library of compounds and identified six xanthones as potential Hsp90-Cdc37 inhibitors. The inhibition of Hsp90 by two of these xanthones was also confirmed by assessing Cdc28 depletion. Future work will be required to identify the mechanism of action, namely whether the compounds are disruptors of the Hsp90-Cdc37 complex or direct HSP90 or Cdc37 inhibitors. These compounds may be used in the development of improved molecules with more potent and selective properties for potential therapeutic use.

Keywords

Protein Folding; Molecular Chaperones; Yeast Screening Model; Hsp90 inhibition; Hsp90-Cdc37 inhibition

Table of Contents

List of Tables

List of Figures

List of Abbreviations

17-AAG	17-N-allyloamino-17-demethoxygeldanamycin / Tanespimycin
ABC	ATP-Binding Cassette
Aha1	Activator of Hsp90 ATPase
Cdc28	Cell division cycle 28
Cdc37	Cell division cycle 37
CDK	Cyclin-dependent kinase
CHIP	Carboxyl terminus of Hsp70-interacting protein
CHX	Cycloheximide
CK2α	Casein Kinase II 2α
CTD	Carboxy-terminal domain
DMSO	Dimethyl sulfoxide
EGFR	Epidermal Growth Factor Receptor
ErbB2	Erb-B2 Receptor Tyrosine Kinase 2
G418	Geneticin
GDA	Geldanamycin
GRP94	95kDa glucose-regulated protein
HIF-1α	Hypoxia inducible factor 1 subunit alpha
HOP	Hsp70-Hsp90 organizing protein
HSF1	Heat shock factor 1
Hsps	Heat shock proteins
Hxk	Hexokinase
IL	Interleukin
LB	Lysogeny Broth
MD	Middle domain

NTD	Amino-terminal domain
OD	Optical Density
OE	Over expression
PCR	Polymerase chain reaction
PDR	Pleiotropic drug resistance
Pgk1	Phosphoglycerate Kinase 1
PINK1	PTEN-induced kinase 1
PKB	Protein kinase B
PPI	Protein-protein interface
PP5	Protein phosphatase 5
SC	Synthetic complete
SDS	Sodium dodecyl sulphate
TBS	Tris-buffered saline
TPR	Tetratricopeptide-containing repeats
TRAP1	Tumour necrosis factor receptor-associated protein 1
WA	Withaferin A
WT	Wild type
Y2H	Yeast Two-Hybrid
YPD	Yeast Peptone Dextrose

1. Introduction

1.1 Protein Folding and Chaperones

Proteins are a versatile and structurally complex class of biomolecules that are responsible for carrying out a wide range of biological functions such as providing cell structure, gene regulation, enzyme catalysis, cellular transport, and response to a multitude of signals. Protein kinases are a highly dynamic class of proteins associated with cell signalling and a plethora of biological processes such as cell cycle regulation and organism development (Taylor et al., 2012). Through the process of protein folding, proteins kinases acquire a three-dimensional structure that provides the necessary stability allowing the proteins to work properly. These proteins need to retain conformational flexibility to maintain their activity, therefore, they are only marginally thermodynamically stable (Hartl et al., 2011). In fact, some proteins - Intrinsically Disordered Proteins (IDPs) - appear to be devoid of any ordered three-dimensional structure and only adopt a specific folding through interaction with determined binding partners (20-30% of all proteins in eukaryotic mammalian cells) (Dunker et al., 2008). For example, aberrant behaviour of the tau and α-synuclein proteins can lead to the formation of fibrillar aggregates associated with neurological diseases such as dementia and Parkinson's disease (Hartl et al., 2011). In the case of protein kinases, loss of stability leads to dysregulation of cellular processes, associated with many diseases including cancer. Therefore, protein kinases have become key therapeutic targets (Zhang et al., 2009). Given the importance that achieving a conformational stable structure has for the different cellular processes, understanding the mechanisms associated with protein quality control and the maintenance of proteome homeostasis (proteostasis) is paramount for cellular and organismal health and has been studied for over half a century (Dill & MacCallum, 2012).

In vitro, unfolded small proteins can very quickly acquire their native state spontaneously, however, larger proteins with multiple domains may require minutes or even hours to fold properly (Hartl et al., 2011). *In vivo*, the folding of the same proteins becomes significantly more difficult due to factors such as higher protein concentration and higher tendency of protein aggregation caused by macromolecular crowding (Hartl et al., 2011). The molecular reactions than ensure the correct protein folding occur thanks to multiple weak non-covalent interactions capable of burying non-polar amino

acid residues in the interior of the protein while maintaining the polar residues in the exterior. Between the unfolded state and the final three-dimensional structure, the protein establishes different intermediate structures and, depending on the protein size, flexibility, and topology, these partially folded states may tend to aggregate due to the exposure of hydrophobic amino acid residues forming either amorphous structures or fibrillar aggregates. In these conditions, pre-existing protein machinery, molecular chaperones, are able to recognize and bind these hydrophobic residues, preventing their exposure to the solvent and allowing the protein to achieve the correct folding (Hartl et al., 2011). The concept of chaperone can be defined as any protein that, by establishing interactions, is able to stabilize or help other proteins acquire a functional active conformation while being absent in the protein's final structure (Hartl & Hayer-Hartl, 2009). Molecular chaperones are crucial regulators of homeostasis. They bind to nascent polypeptides, stabilizing and helping them to fold correctly, helping in the assembly and disassembly of macromolecular complexes, and mediating the refolding of misfolded proteins (Ellis, 2007). Moreover, molecular chaperones reduce the danger of protein aggregation by activating the ubiquitin-proteasome system (UPS) and the autophagy system to eliminate misfolded and aggregated proteins (Hartl et al., 2011; Trepel et al., 2010).

The major chaperone classes consist in a large family of highly conserved and ubiquitously expressed proteins named heat shock proteins (Hsps) (Hartl et al., 2011). The heat shock proteins are commonly known as stress proteins due to being dramatically upregulated under stress conditions such as hyperthermia, irradiation, and toxins, which lead to protein aggregation (Xiao & Liu, 2020). The different Hsps have been classified in five different classes based on their molecular weight - Hsp60, Hsp70, Hsp90, Hsp104 and small Hsps. Structurally, there are also some differences of note between the different classes of Hsps: Hsp60s form a barrel-like Anfisen cage; Hsp70s and the small Hsps establish "clamps" devised to interact and protect exposed hydrophobic amino acid residues in their proteins; Hsp90s adopt multidomain v-shaped structures; and Hsp104s consist of hexameric rings (Bascos & Landry, 2019).

1.2 Heat Shock Protein 90 (Hsp90)

The 90 kDa Hsp is one of the most conserved Hsps and it is ubiquitously present in wide range of living organisms (except archaea), from bacteria to eukaryotes. Its role surpasses that of simple stress response and it can interact, in different degrees, with more than 400 client proteins, including protein kinases (e.g., Raf), transcription factors (e.g.,HIF-1α), E3-ligases (e.g., cullin 3), and steroid hormone receptors (e.g., oestrogen receptor), being therefore associated with signal transduction, receptor maturation, the innate and adaptive immunity and protein trafficking (Farid Ahmad Siddiqui et al., 2021; Taipale et al., 2010). Hsp90 represents the most widely studied and the more clinically significant family of chaperones due to its involvement as a crucial facilitator of oncogene addiction and cancer cell survival (Trepel et al., 2010). In order to establish a connection with the different client proteins, Hsp90 interacts with over 20 co-chaperones (non-client binding proteins) such as Cdc37, TTC4 and Sgt1 (Biebl et al., 2020). Through this interaction, the co-chaperones modulate its biochemical activities and allow it to achieve proper client recognition. However, due to the transient nature of complexes formed by Hsp90, the wide range of client proteins and the participation different co-chaperones in folding process, the Hsp90's mechanistic functions remain unclear (Prodromou & Bjorklund, 2022).

Higher eukaryotes possess up to four Hsp90 homologs that are compartment specific: the cytosolic Hsp90A, the mitochondrial tumour necrosis factor receptor-associated protein 1 (TRAP1), the endoplasmic reticulum homolog 95kDa glucose-regulated protein (GRP94) Hsp90B and the chloroplast Hsp90C (Zhang et al., 2022). Through comparative analysis of Hsp90 sequences, it appears that the eukaryotic families have evolved from the high temperature protein G (HtpG) present in most bacteria. However, this family of Hsp90 is non-essential in non-stressful conditions unlike the eukaryotic Hsp90 (Taipale et al., 2010).

The mammalian cytosolic Hsp90 represents 1-2% of total protein levels in the cytoplasm (Taipale et al., 2010) and can be divided into two isoforms, the Hsp90α and the Hsp90β. Despite the 85% similarity between the two isoforms, they possess different functions in the cell. While Hsp90α (inducible isoform) is secreted extracellularly and associated with tumour growth (invasion, angiogenesis, and metastasis) (Vartholomaiou et al., 2017), Hsp90β (constitutive isoform) is linked to antiapoptotic functions of B-cell lymphoma 2 (Bcl2) (S. Li et al., 2017) . Under stress conditions, the heat shock factor 1 (HSF1) increases the expression of the inducible cytosolic Hsp90 (Hsp90α) (Taipale et al., 2010). HSF1 is a Hsp90 client and, when a stress response is not required, the

transcription factor is kept in a complex with Hsp90 and Hsp70 as a part of Hsp90 self-regulating mechanism (Chakraborty & Edkins, 2020) . In the case of the human Hsp90α, a multitude of other transcription factors control the increase of chaperone levels in response to stress conditions. For instance, upon interleukin-6 (IL-6) stimulation, it can be induced by NF-IL6β and signal transducer and activator of transcription 3 (STAT3), whereas Interferon-γ (IFN-γ) stimulates signal transducer and activator of transcription 1 (STAT1) leading to an increased Hsp90α expression (Prodromou, 2016) . The transcription can also be induced by the binding of nuclear factor-kB subunit p65 to a consensus sequence in the Hsp90 promoter (Prodromou, 2016). In addition to transcriptional regulation, Hsp90α is regulated through several post-translational modifications, such as phosphorylation and acetylation which can modify the interaction of Hsp90 with co-chaperones and client-proteins (Zhang et al., 2022) .

Lower eukaryotes, such as *S. cerevisiae,* possess only cytosolic Hsp90 forms that are essential for cell viability. Regarding the amino acid sequence, the two yeast cytosolic isoforms*,* Hsp82 and the Hsc82, share 97% identity among themselves and about 60% identity with the cytosolic mammalian Hsp90 (Johnson, 2012). Hsc82 is the constitutive isoform that is expressed at high levels under normal cell conditions, being moderately induced in response to heat stress. On the other hand, Hsp82 is highly induced in response to heat stress, achieving levels similar to Hsc82, and represents the more stable and efficient isoform (Girstmair et al., 2019). However, despite the different degrees of expression, both isoforms appear to possess specific important functions in the respective cell conditions in which they are predominant (Girstmair et al., 2019) .

1.3 Hsp90 Structure

All Hsp90 homologs range in size between 588 to 854 amino acids and consist of dimers with high intrinsic structural flexibility that have weak ATPase activity (Johnson, 2012) and are related to ATPases such as the MutL family of DNA mismatch repair proteins, DNA gyrase and type II and type IV topoisomerases (Hoter et al., 2018). This flexibility has hindered the structural analysis conducted throughout the years, however, Hsp90's structure has been characterized in bacteria, yeast and in mammals (Taipale et al., 2010). In general, the protein's architecture remains similar throughout the different species and most identified differences relate to subdomain rotations (Taipale et al., 2010). The basic structure that comprises each dimer of the cytosolic Hsp90 consists of

an amino-terminal domain (NTD) that is connected through a flexible charged linker to the middle domain (MD), followed by the carboxy-terminal domain (CTD) (Taipale et al., 2010). The NTD has the highest degree of conservation (approximately 85%) and possesses a nucleotide binding site (adenosine specific) that binds ATP (Hoter et al., 2018). This ATP-binding site is comprised of α- and β-sandwich motifs (Jackson, 2013) and possess several conserved amino acid residues that form a molecular "lid" able to close upon ATP-binding (Wang et al., 2021). Besides being able to bind ATP, the interaction established between the NTD of the two monomers that comprise the Hsp90 dimeric structure is positively associated with the chaperone activity (Cunningham et al., 2008). The charged linker that connects the NTD to the middle domain is only present in eukaryotic Hsp90. This highly charged linker can possess different lengths and be comprised of different amino acid sequences. The linker's flexibility allows the chaperone to adapt its structure to accommodate an interaction with a myriad of different client proteins while counteracting the crowded cellular environment (Hoter et al., 2018). Further studies are required to determine the extent of its influence in Hsp90's activity, however, it has been found that mutations impair both client activation and regulation by co-chaperones (Hainzl et al., 2009). The middle domain is comprised of αβα motifs connected by α-helices and possesses hydrophobic patches and amphipathic protrusions that are essential for the interaction with client proteins and co-chaperones (Taipale et al., 2010). Moreover, it also binds the γ-phosphate of ATP bound in the NTD modulating the chaperone ATPase activity (Peng et al., 2022). The CTD is constituted by a mixture of α- and β- domain and possesses the least conserved amino acid sequence of the protein (Taipale et al., 2010). This domain has three different binding sites, one for the binding of calmodulin, one that allows for Hsp90 homodimerization and one that opens upon ATP binding and can serve as an allosteric regulator of the NTD ATPase activity (Hoter et al., 2018). Despite being less conserved, the CTD possesses a conserved sequence of 5 amino acids (Met-Glu-Glu-Val-Asp), the MEEVD motif, which binds to helical hairpins containing approximately 34 amino acid residues, named tetratricopeptide-containing repeats (TPR-domain), present in co-chaperones such as HOP (Hsp70-Hsp90 organizing protein) and immunophilins, playing an important role in mediating co-chaperone interaction (Hoter et al., 2018).

As previously stated, Hsp90 possesses a highly flexible structure that is intrinsic to its activity. This allows it to undergo major transient conformational alterations during its ATPase cycle. When no nucleotide is bound to the chaperone, it exists in an equilibrium of states that vary between very open conformations and closed ones. Unlike what happens with other chaperones, the binding of ATP does not restrict Hsp90 into a

single conformation as Hsp90 still maintains an equilibrium of several conformational states, it simply starts favouring a more closed state where the chaperone is active (Taipale et al., 2010). However, the equilibrium established between the different conformations is different depending on the species. For instance, while the human Hsp90 only transiently assumes the closed conformation, the yeast Hsp90 almost entirely adopts a closed conformation (Verba & Agard, 2017). In the absence of nucleotide binding, Hsp90 exists in a variety of open state conformations with dimer formation only in the CTD. Upon ATP binding in the NTD, a series of conformational changes occur, where several conserved amino acid residues present in the NTD translocate over the binding pocket attaching to the NTD of the other Hsp90 monomer, twisting and forming a compact symmetric homodimer stabilized by the action of different co-chaperones (Hoter et al., 2018; Verba & Agard, 2017). Through the hydrolysis of the ATP molecules present in the NTD, the chaperone first acquires an asymmetric conformation and then a compact transient conformation where ADP is bound. Finally, ADP and inorganic phosphate (Pi) are released and Hsp90 returns to its initial equilibrium of open state conformations (**Fig. 1**) (Verba & Agard, 2017). The major conformational changes that take place during the ATPase cycle represent the rate limiting steps because they are much slower than the hydrolysis of ATP (Taipale et al., 2010).

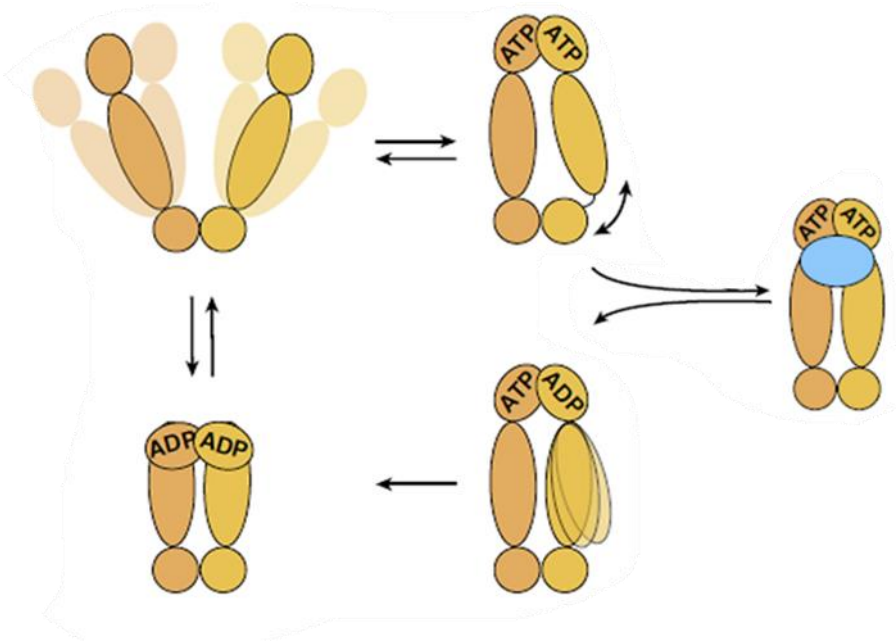

***Figure 1*- Hsp90 ATPase cycle.** In the absence of nucleotide binding Hsp90 remains in an equilibrium of open state conformations. Upon nucleotide binding, Hsp90 acquires closed conformation. Through ATP hydrolysis ADP and Pi are released and the chaperone returns to an open state conformation. Adapted from *Verba KA, Trends Biochem sci, 2017*

1.4 Hsp90 Co-chaperones

In order to modulate its biochemical activity and tackle distinct cellular conditions, Hsp90 establishes complexes with over 20 co-chaperones (**Fig. 2**) (Taipale et al., 2010). This modulation can occur through four distinct methods. Co-chaperones can stimulate or inhibit Hsp90 ATPase activity, coordinate interaction with other chaperones, grant the chaperone complex specificity to certain protein clients and, in a more general way, influence different aspects of the ATPase cycle (Taipale et al., 2010).

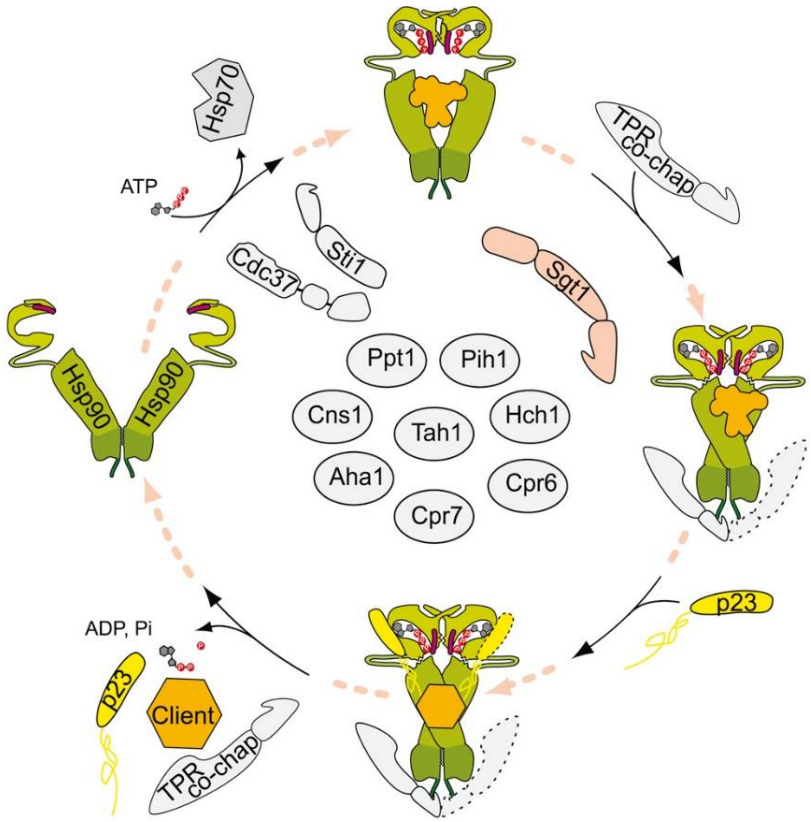

Figure 2- Hsp90 conformational flexibility allows for the interaction with different co-chaperones. Examples of Hsp90 co-chaperones in mammalian cells is shown. Adapted from *Sahasrabudhe P., Moll. Cell, 2017*

The largest class of co-chaperones are a group of co-chaperones possessing one or more TPR domains that bind to the MEEVD motifs located on the Hsp90 CTD. TPR domains are very widespread, thus the co-chaperones containing it are themselves very diverse in structure and function (Prodromou & Bjorklund, 2022). Examples of TPR containing co-chaperones are WISp49 and HOP, associated with client protein recruitment, the translocase of outer mitochondrial membrane 70 (TOM70), associated with the recruitment of Hsp90 to other multiprotein systems, the carboxyl terminus of Hsp70-interacting protein (CHIP), an E3/E4-ubiquitin ligase, the protein phosphatase 5 (PP5), a serine/threonine phosphatase, and the tetratricopeptide repeat protein 2 (TPR2), associated with the recycling of substrates through multichaperone machinery (Prodromou & Bjorklund, 2022; Taipale et al., 2010). The varied co-chaperones possess specificity to different Hsp90 conformations, therefore, different Hsp90-co-chaperone complexes are formed throughout the different stages of the Hsp90 ATPase cycle (Prodromou & Bjorklund, 2022). For instance, while Sgt1 and Hop1/Sti1 bind to the open state conformation of Hsp90, other co-chaperones, such as the activator of Hsp90 ATPase (Aha1) and p23, bind to the closed conformation (Sahasrabudhe et al., 2017).

Regarding the different roles of the co-chaperones on Hsp90 regulation, Aha1 and Ppt1 act as remodelling chaperones while Hop1/Sti1, cell division cycle 37 (Cdc37) and Sgt1 are responsible for client recruitment (Sahasrabudhe et al., 2017). Another important aspect of Hsp90 regulation by co-chaperones is the ability to induce the activation or inhibition of the ATPase cycle. Co-chaperones such as Aha1 and Cpr6 activate the ATPase cycle by accelerating Hsp90's early conformation transitions (Taipale et al., 2010). Cdc37, Hop1/Sti1 and p23 are associated with the recruitment of client proteins and favour the inhibition of the ATPase cycle in order to facilitate client protein loading and the formation of mature complexes (Prodromou & Bjorklund, 2022; Reidy et al., 2018) .

Cdc37 is a cell division cycle control protein that was initially identified as a phosphoprotein component of Hsp90 complex with the oncogene v-Src. It functions as an adaptor/scaffold protein allowing Hsp90 to interact a series of protein kinases (Czemeres et al., 2017). In fact, approximately 60% of the human kinome is maintained through interaction with the Hsp90-Cdc37 chaperone complex (Verba & Agard, 2017). Structurally, it possesses three distinct domains, an NTD, a central domain, and a CTD (Czemeres et al., 2017). In order to connect the different kinase clients to Hsp90, Cdc37 arrests the ATPase cycle by inhibiting various structural rearrangements. Cdc37's central and CTD bind Hsp90's NTD through several hydrophobic interactions established between Cdc37 large helical domain and the conserved molecular "lid" present in Hsp90 NTD (Pearl & Prodromou, 2006). Blocking the "lid" in an open conformation prevents it to close over the ATP molecule and impedes the ATPase cycle to start. Moreover, when bound to Hsp90's NTD, Cdc37 prevents the interaction between the ATP-binding pocket and the catalytic loop present in Hsp90 middle domain. Lastly, it inhibits NTD dimerization required to achieve a closed state conformation for ATP hydrolysis. Cdc37 NTD possesses the majority of its kinase-binding activity and interacts with the different kinase clients (Keramisanou et al., 2016; Verba et al., 2016). The Hsp90-Cdc37 chaperone complex is regulated by phosphorylation by Yes and Casein Kinase II 2α (CK2α) kinases (Verba & Agard, 2017; Xu et al., 2012).

In order to recognize and associate with client kinases, Cdc37 is phosphorylated by CK2α (Serwetnyk & Blagg, 2021). Afterwards, at the start of the Hsp90-Cdc37 kinase cycle, Cdc37 NTD binds an unfolded kinase. Once this interaction is established, Cdc37's central and CTD interact with the NTD of an open state Hsp90 and PP5 dephosphorylates Cdc37, stabilizing the client protein for transfer to Hsp90 (Serwetnyk & Blagg, 2021). Upon the binding of ATP, a conformational change is induced in the Hsp90 structure, and it closes around the unfolded kinase, translocating Cdc37 to the middle domain. The ATP is hydrolysed, and the chaperone complex aids the kinase to acquire the proper folding. Finally, the folded kinase, Cdc37, and ADP plus inorganic phosphate are released (**Fig. 3**) (Verba & Agard, 2017).

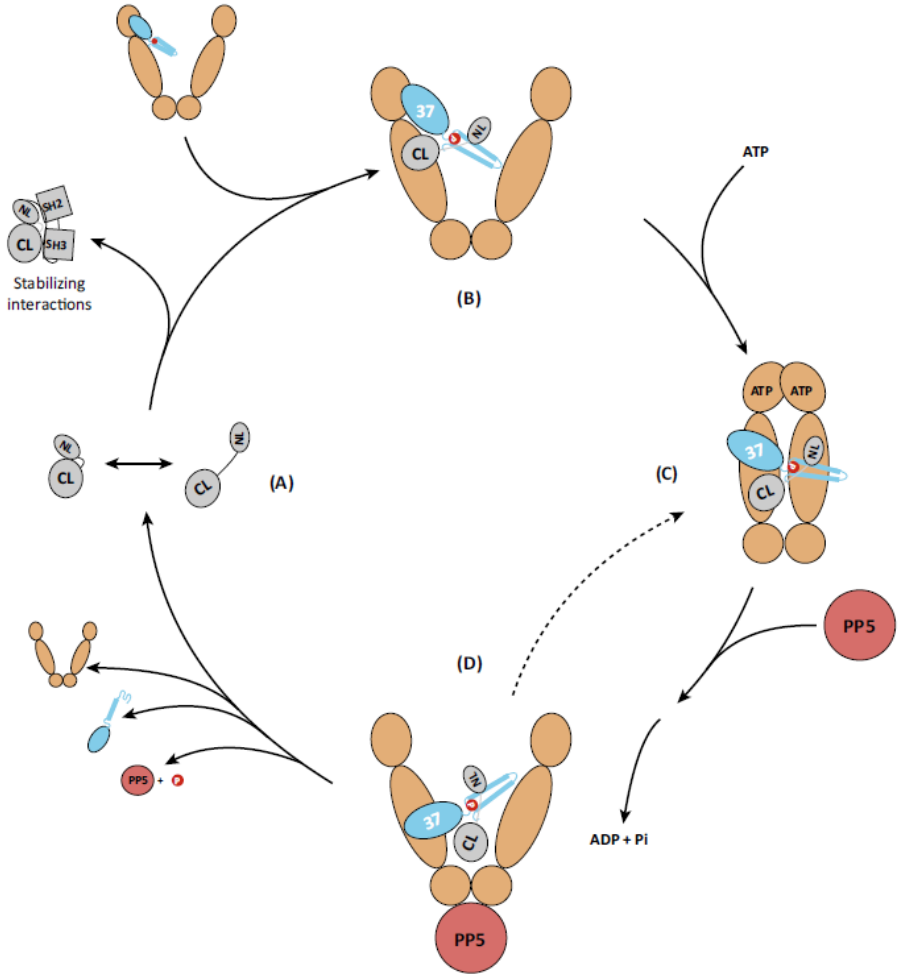

Figure 3- Hsp90-Cdc37 kinase folding cycle. Upon phosphorylation by CK2α, Cdc37 NTD binds an unfolded kinase. Afterward, Cdc37 central and CT domains interact with Hsp90 NTD and PP5 dephosphorylation of Cdc37 prepares client kinase for Hsp90 transport. Through ATP binding and subsequent hydrolysis Hsp90 closes around the unfolded kinase and aids it to achieve proper folding. Cdc37 ADP, organic phosphate and the folded kinase are released. Adapted from *Verba KA, Trends Biochem sci, 2017.*

Examples of kinases associated with the Hsp90-Cdc37 chaperone complex are the epidermal growth factor receptor (EGFR), the family of non-receptor tyrosine kinases Src, the serine/threonine kinase B-Raf, the cyclin-dependent kinase 4 (CDK4) and the cyclin-dependent kinase (Cdc28/CDK1) (Li et al., 2018). Malfunctions in the Hsp90-Cdc37 chaperone complex can give rise to neurodegeneration through the abnormal stabilization of kinases such as the PTEN-induced kinase 1 (PINK1) and the leucine rich repeat kinase 2 (LRRK2) (Gracia et al., 2019), while maintenance of ErbB2 can lead to oncogenesis (Verba & Agard, 2017). Henceforth, successful manipulation of this chaperone complex may provide an effective therapeutic approach.

Yeast possess orthologs of Hsp90 co-chaperones that generally play similar functions in regulating Hsp90 (Johnson, 2012). Among the different co-chaperones present in yeast, only Cdc37, Cns1 and Sgt1 are essential for cell survival (Biebl et al., 2020). Yeast Cdc37 has 19% similarity to its human ortholog (MacLean & Picard, 2003).

1.5 Hsp90 Client Proteins

A client protein can be defined as one that simultaneous establishes a physical interaction with the chaperone and whose activity decreases (usually through proteasome degradation) upon chaperone inhibition. Hsp90 occupies a vital place in the regulation of multiple cellular processes by interacting with different client proteins such as multiple nuclear hormone receptor complexes, transcription factors, chromatin proteins, the telomerase reverse transcriptase (TERT) and the endothelial nitric oxide synthase (eNOS) (Taipale et al., 2010; Tariq et al., 2009). However, despite the involvement with all kinds of proteins, most of Hsp90 clients consists of either nuclear steroid receptors or kinases (Taipale et al., 2010). However, the process of client recognition is still unclear and common amino acid sequences or structural characteristics shared between the different clients are unknown (Taipale et al., 2010). Alternatively, it has been postulated that, instead of the primary sequence of proteins, Hsp90 recognizes certain conformations or client protein stability (Li & Buchner, 2013). This client recognition conundrum can be associated with the fact that, despite being a useful concept, the interaction between a protein and a chaperone cannot be reduced to a simple client and non-client classification. Instead, it is more appropriate to establish where a certain protein lies in the continuum of chaperone dependence (Verba & Agard,

2017). For instance, while EGFR only transiently associates with Hsp90, ErbB2 forms a stable complex with the chaperone (Xu et al., 2005). Moreover, other extrinsic factors such as temperature, cell tissue type, alternative splicing, cell signalling events, post-translational modifications, the presence of other proteins and even environmental signals influence the interaction between a specific protein and Hsp90 (Taipale et al., 2010). Given the Hsp90 ability to bind and stabilize several mutant protein kinases, and the pleiotropic effects suffered by other proteins in case of Hs90 disruption, further studies regarding the interactions established among chaperone, co-chaperone and client protein are required. In yeast Hsp90 approximately 20% of proteins are influenced by Hsp90's activity (Taipale et al., 2010).

When client proteins fail to achieve the correct folding after successive chaperone binding and release attempts, Hsp90 may passively or actively promote proteasomal protein degradation by establishing a complex with ubiquitin ligases (e.g., the E3 ubiquitin ligase CHIP) (McClellan et al., 2005; Taipale et al., 2010).

1.6 Hsp90 and therapy

As previously stated, Hsp90 activity is highly associated with human health by playing an important role not only in the maintenance of vital cellular processes but also through its inherent activity in the progression of diseases such as cancer, neurodegeneration, cystic fibrosis, viral disease, parasitic disease and fungal disease (Devaney & Gillan, 2016; Gracia et al., 2019; Lamoth et al., 2016; Pearl, 2005; Wang et al., 2006; Wang et al., 2017). Moreover, it is also associated with the ageing process (Fuhrmann-Stroissnigg et al., 2017).

Hsp90 is associated with a wide range of client proteins that have been found overexpressed or mutated in cancer. Through the process of oncogenesis, many Hsp90 client proteins are associated with characteristics developed and exhibited by all cancers, the hallmarks of cancer (Hanahan & Weinberg, 2000). Proteins such as Raf-1 and Her-2 are associated with the ability of cancer cells to produce their own cell growth signals while proteins such as Cdk4 and Cdk6 can allow them to grow insensitive to anti-growth signals produced by the surrounding cells. Together these alterations allow for a fast and dysregulated cancer cell growth. Proteins such as p53 and survivin allow cancer cells to evade apoptosis, whereas the hypoxia inducible factor 1 subunit alpha (HIF-1α)

and the vascular endothelial growth factor (VEGFR) are involved in the process of angiogenesis, crucial to assure the supply of nutrients to the microtumour environment. The state of replicative longevity is associated with client proteins telomerase and the forkhead box M1 (FoxM1), and the ability to invade other tissues and metastasize is linked to proteins such as c-Met and the protein arginine methyltransferase 5 (Prmt5). Furthermore, the arrestin beta 1 (Arrb1) and arrestin beta 2 (Arrb2) are implicated with the dysregulation of cellular energetics, and the interleukin-1 receptor-associated kinase 3 (Irak3) contributes to immune response evasion. Lastly, genome instability is promoted by the MAF BZIP transcription factor G (Mafg) and the NIMA related kinase 8 (Nek8), and tumour inflammation by IL-6 and IL-8 (Serwetnyk & Blagg, 2021). Since a large number of oncoproteins either depend on Hsp90 interaction or form chaperone complexes with it and Hsp90 levels increase 2 to 10-fold in tumour cells (Li & Buchner, 2013), the chaperone is an important target and the development of inhibitors represents an attractive therapeutical strategy (Xiao & Liu, 2020).

The chaperone complex Hsp90-Cdc37 has been linked to protein aggregation and progression of different neurodegenerative diseases (Gracia et al., 2019). Alzheimer's disease results from the accumulation of protein aggregates rich in β-amyloid (Aβ) between neurons and the formation of intraneuronal tangles made up by tau protein (Gracia et al., 2019). It has been found that Hsp90 client kinases such as cyclin-dependent kinase 5 (CDK5) and protein kinase B (PKB) are associated with the production and stabilization of Aβ (Castro-Alvarez et al., 2015; Yang et al., 2018). Moreover, not only is tau protein stabilized through interaction with Hsp90-Cd37 complex but the reduction of Cdc37 levels is also linked with tau elimination (Jinwal et al., 2011). Parkinson disease is characterized by a progressive decline in both cognitive and motor abilities associated with mitochondrial dysfunction, oxidative stress, and the aggregation of misfolded α-synuclein that leads to the formation of Lewy bodies (Gracia et al., 2019). The Hsp90-Cdc37 complex is associated with α-synuclein aggregation by regulating its phosphorylation through potential interaction with α-synuclein kinase regulators such as the Src family and casein kinase (Gracia et al., 2019). Regarding mitochondrial dysfunction, Hsp90-Cdc37 chaperone complex role has been implicated in the regulation, processing, and subcellular localization of Pink1, which is essential for mitochondrial quality control (Wang et al., 2021). Huntington's disease results from an autosomal dominant mutation in the huntingtin gene and manifests through the loss of cognition and motor functions induced by neurotoxic aggregates (Gracia et al., 2019). Notably, inhibition of Hsp90 leads reduced mutant huntingtin aggregation (Wang & Lu, 2022).

1.6.1 Hsp90 NTD Inhibitors

The development of Hsp90 inhibitors started with the discovery that the natural antibiotic Geldanamycin (GDA) inhibits Hsp90. GDA is a 1,4-benzoquinone ansamycin (Li & Buchner, 2013) isolated from *Streptomyces hygroscopicus* that is able to competitively bind to the ATP binding site in Hsp90 NTD, inhibiting the ATPase cycle and the associated conformational changes required for Hsp90 activity (Siddiqui et al., 2020). Despite having strong antiproliferative activity, it was shown that its unstable structure, poor solubility, and hepatoxicity rendered the compound unusable for clinical trials (Xiao & Liu, 2020). Radicicol (or monorden) is another natural antibiotic that can inhibit Hsp90. It is a 14-membered macrolide isolated from *Monosporium bonorden (Li et al., 2012) . In vitro,* Radicicol possesses high toxicity and acts as a nucleotide-mimicking compound that has higher affinity to the ATP binding site than ATP, inhibiting its association with Hsp90 (Khandelwal et al., 2016) . However, *in vivo,* due to biologic structural instability, it does not show any activity (Xiao & Liu, 2020). Through chemical optimization of these natural compounds, a myriad of other new Hsp90 NTD inhibitors have been obtained.

Manipulation of geldanamycin through the replacement of the methoxy group with an allylamino group allowed for the formation of 17-N-allyloamino-17-demethoxygeldanamycin (or tanespimycin) (17-AAG) that showed improved hydrophilicity and bioavailability in comparison to GDA (Li & Buchner, 2013). However, despite entering clinical trials in 1999, it failed due to high toxicity, off-target effects, variable pharmacokinetics and polymorphic metabolism by enzymes (Banerji et al., 2005; Eccles et al., 2008). In order to further develop solubility, 17-Dimethylaminoethylamino- 17-demethoxygeldanamycin (or alvespimycin) (17-DMAG) was also developed but it also showed dose-limiting side effects (Xiao & Liu, 2020). Further structure manipulation led to the formation of another more soluble geldanamycin analogue, the 17-AAG hydroquinone Retaspimycin hydrochloride (IPI-504) (Sequist et al., 2010). Multiple small semisynthetic molecules possessing a resorcinol motif found in radicicol have been developed in order to improve radicicol pharmacokinetics (Eccles et al., 2008). The first molecule to be identified was an isoxazole amide dubbed luminespib (or NVP-AUY922) that binds to Hsp90 NTD and inhibits the chaperone, resulting in reduced human tumour cells proliferation (Lian et al., 2017). Other resorcinol based compounds such as AT13387, KW-2478 and STA-9090 have also been developed and are in clinical trials (Xiao & Liu, 2020). A compound possessing both the

radicicol resorcinol ring the geldanamycin quinine ring connected through an amide linkage has also been developed. This chimeric compound, radamide, has shown to be able to inhibit Hsp90 ATPase activity and induce the degradation of several client proteins in breast cancer cells (Clevenger & Blagg, 2004).

Another class of Hsp90 NTD inhibitors was discovered through rational design. These inhibitors target the entry region of the ATP binding pocket, and consist of purine-based inhibitors (Taldone & Chiosis, 2009). The first identified synthetic Hsp90 inhibitor to possess a purine scaffold was 9-butyl-8-(3,4,5-trimethoxybenzyl)-9H-purin-6-amine (PU3) (Trendowski, 2015) and was shown to have similar phenotypic effects to GDA in breast cancer cells (Taldone & Chiosis, 2009). Since this discovery, further efforts were made to improve the potency and chemical properties of compounds containing the purine-scaffold (Trendowski, 2015). The first of these compounds to be submitted for clinical tests was a prodrug activated through dephosphorylation named BIIB021. Other purine scaffold containing inhibitors such as Debio0932, MPC-3100, PU-H71, and CUDC-305 have since been developed (Li et al., 2018; Xiao & Liu, 2020).

Other Hsp90 NTD inhibitors can be based of different scaffolds. For instance, SNX-5422 is a highly selective orally active Hsp90 inhibitor characterized by having a benzamide scaffold (Fadden et al., 2010). Examples of other inhibitors containing benzamide scaffold developed from SNX-5422 are TAS-116 and XL-888 (Xiao & Liu, 2020). Compounds such as Hsp990 that contains a dihydropyridopyrimidinone scaffold represent yet another type of synthesized Hsp90 NTD inhibitors (Xiao & Liu, 2020).

To date, no Hsp90 inhibitory compound has been approved by FDA and most compounds have failed clinical trials (Serwetnyk & Blagg, 2021). All Hsp90 inhibitors that have been successful in reaching clinical trials target the ATP-binding site located in Hsp90 NTD (Xiao & Liu, 2020). The problem associated with this type of inhibition is correlated to the fact that, as it has been previously stated, all Hsp90 isoforms share at least 85% sequence identity in the ATP-binding site. Therefore, this targeting approach ultimately leads to multiple off target effects, such as gastrointestinal, cardiac, and ocular toxicities (Hong et al., 2013). Moreover, targeting the Hsp90 NTD induces a strong pro-survival heat shock response through the activation of HSF1 that induces the overexpression of antiapoptotic heat shock proteins such as Hsp72, Hsp27, and even Hsp90 itself (Piper & Millson, 2011; Workman et al., 2007).

1.6.2 Hsp90 CTD Inhibitors

The development of inhibitors that target Hsp90 CTD and even both Hsp90 NTD and CTD has also resulted in the discovery/synthesis of several compounds over the years (Xiao & Liu, 2020). Hsp90 CTD inhibition can be divided into two categories, one related to inhibitors that target the nucleotide binding site (Siddiqui et al., 2020). Despite not displaying any ATPase activity, the CTD possesses a nucleotide binding site that overlaps with its dimerization domain and is essential for Hsp90 rearrangement upon ATP binding (Serwetnyk & Blagg, 2021). Novobiocin was the first natural product to be identified as a CTD inhibitor. It is a coumarin antibiotic isolated from multiple *Streptomyces* strains and is able to interact with Hsp90 CTD ATP-binding pocket, not only disrupting the chaperone ability to dimerize but also inducing conformational changes that ultimately lead to the proteasomal degradation of client proteins such as Erb-B2 Receptor Tyrosine Kinase 2 (ErbB2) and Raf-1 through ubiquitination (Donnelly & Blagg, 2008; Li et al., 2012). However, the effect of novobiocin is weaker than Hsp90 NTD inhibitors and further modifications are prone to enhance its activity (Li et al., 2012; Xiao & Liu, 2020). Epigallocatechin-3-gallate (EGCG) is a polyphenol catechin that binds directly (or adjacently) to CTD ATP-binding site, inhibiting Hsp90 dimerization and disrupting the association with several co-chaperones such as p23 and leading to the degradation of protein clients such as PKB, Cdk4 and Her-2 (Li et al., 2012). The chemotherapeutic cisplatin has also demonstrated the ability to bind to CTD and interfere with nucleotide binding, however, its usage is limited by the development of acquired resistance (Donnelly & Blagg, 2008).

The other category of CTD inhibitors engage different allosteric sites present in Hsp90 CTD (Siddiqui et al., 2020). Withaferin A (WA) is a natural compound obtained from the medicinal plant *Withania somnifera* that binds to a cysteine residue present in Hsp90 CTD, inhibiting its activity through an ATP independent mechanism (Wang et al., 2021). WA has previously shown strong antitumour activity both *in vitro* and *in vivo* by inducing client protein degradation (Yu et al., 2010). Moreover, withaferin A appears to specifically inhibit the formation of Hsp90-Cdc37 complex (Wang et al., 2021). Similarly, celastrol, another natural pentacyclic quinone methide triterpene that has been isolated from root extracts of *Tripterygium wilfordi,* is able to bind Hsp90 CTD and allosterically modulate the chaperone ATPase activity. It also specifically disrupts the Hsp90-Cdc37 chaperone complex and possesses potent anticancer activity (Wang et al., 2021). When compared with other inhibitors such as novobiocin, the CTD allosteric inhibitors appear to have a higher inhibitory effect (Siddiqui et al., 2020).

Panaxynol (or falcarinol) is a Hsp90 inhibitor that has shown similar affinity to both NTD and CTD. It possesses strong antitumour activity and is able to induce the proteasomal degradation of multiple Hsp90 clients without inducing a heat shock response typical of NTD inhibition (Xiao & Liu, 2020).

1.6.3 Direct protein-protein interface (PPI) Inhibitors

More specific strategies that target direct protein-protein interfaces (PPI) and prevent the formation of functional heteroprotein complexes have been conducted in order to target the interaction between Hsp90 and a specific co-chaperone (Serwetnyk & Blagg, 2021).

As it has been previously stated, Cdc37 is a very important Hsp90 co-chaperone that interacts with approximately 300 client proteins, most of which kinases (Serwetnyk & Blagg, 2021). Besides celastrol and withaferin A, other compounds have been developed to specifically disrupt the Hsp90-Cdc37 interaction. Derrubone is a natural prenylated isoflavenoid isolated from *Derris robusta* that stabilizes Hsp90-Cdc37 complex hindering the progression through the protein folding cycle (Hadden et al., 2007). It is capable of inducing strong cell growth inhibition and Her-2, Raf-1 and PKB degradation in human breast cells (Li et al., 2012; Serwetnyk & Blagg, 2021). Platycodin D is a saponin extracted from *Radix Platycodonis* that possesses immunoregulatory, anticancer and anti-atherogenic activities (T. Li et al., 2017). Platycodin D blocks the formation of the Hsp90-Cdc37 complex without inducing heat shock response and reduces the levels of Hsp90-dependent protein kinases such as EGFR and Her-2 (T. Li et al., 2017; Siddiqui et al., 2020). FW-04-806 (conglobatin) inhibits the growth of human myelocytic leukaemia. Despite binding to Hsp90 NTD, FW-04-806 does not affect ATP-binding (Serwetnyk & Blagg, 2021). Instead, it disrupts the interaction established in Hsp90-Cdc37 complex and leads to the degradation of Her-2, Raf-1 and PKB levels without blocking transcription (Huang et al., 2014). Elaiophylin is a structurally similar to conglobatin A and has a wide range of biological activities such as antibiotic, antiviral, antifungal, immunosuppressive and anticancer (Gui et al., 2019). Elaiophylin is able to interfere with the interaction established between Hsp90 NTD and Cdc37 and lead to the dose dependent decline of client proteins such as PKB, Extracellular signal-regulated kinase 1 (ERK1) without affecting the levels of Hsp70 and Hsp90 (F. A. Siddiqui et al., 2021). Other examples of Hsp90-Cdc37 PPI inhibitors are compounds such as gambogic acid, kongesin A, sulphoraphane and DCZ3112 (Serwetnyk & Blagg, 2021).

Other PPI inhibitors have been developed to target the interaction between Hsp90 and multiple important co-chaperones. For instance, TL-2-8, SEW84 and HAM-1 target the interaction between Hsp90 and Aha, an important activator of Hsp90 ATPase activity. Moreover, compounds such as Y-632, 7-Azapteridines and some peptide-based disruptors target the complex formed by Hsp90 and HOP, associated with client protein recruitment from Hsp70. Perifosine and 17-DMCHAG disrupt the interaction between Hsp90 and survivin, associated with cell survival through the regulation of mitosis and the inhibition of apoptosis. The interaction between Hsp90 and p23 can be targeted by PPI inhibitors such as ailanthone, cucurbitacin D, CP9 and gedunin (Serwetnyk & Blagg, 2021).

1.7 Yeast Model

In previous sections, the conservation of certain proteins and signalling pathways between human and yeast have been highlighted. Indeed, due to a high degree of conservation of cellular processes, the yeast model provides a model in which different potential drug inhibitors can be identified while simultaneously providing information regarding compound stability or cellular toxicity (Hughes, 2002). Furthermore, as a microorganism, yeast presents fast and inexpensive growth, allowing for the study of drug effects in a short time, in both solid and liquid simple medium, and possesses moderate resistance to solvents, accelerating the first stages of drug discovery (Hughes, 2002; Simon & Bedalov, 2004). Moreover, human proteins that are not conserved can be expressed in yeast cells allowing for humanized target yeast-based assays to be conducted. Yeast-based assays provide several advantages regarding the conditions in which a specific experiment is being performed. Yeast is advantageous over biochemical methods since it requires no purification of the target protein, which remains in its physiological milieu, associated with the proper cellular co-factors that allow a native conformation. Furthermore, when studying intracellular targets, the tested compounds will be required to pass into the cell through yeast plasma membrane and, if successful, they most likely will also be able to pass through the membrane of mammalian cells. Lastly, the self-replicating ability allows for constant cell renewal and expansion in comparison with *in vitro* systems (Hughes, 2002).

A high number of proteins conserved from yeast to human are associated with cellular processes such as cell division, DNA synthesis/repair and cell metabolism, and mutations in those proteins have been implicated in cancer and other diseases. The

simplicity of yeast genetic manipulation when compared to higher eukaryotes allow for the introduction of these mutations in the yeast genome so that its effects can be studied in a much more accelerated and simplified manner (Hughes, 2002). Moreover, through further genetic manipulation, specific mutation pairs capable of inducing synthetic lethality could be found. This may provide a highly specific targeted therapy resulting in a much less toxic alternative to other drugs administered in chemotherapy (Hughes, 2002). This genetic plasticity specially pontificates the yeast as a valuable model and allowed for the development of multiple yeast-based screening assays such as the yeast two-hybrid. These assays take advantage of well-developed array of tools such as plasmid systems, a vast and well established selection of markers based on amino-acid prototrophy and drug resistance (Hughes, 2002).

The major drawback associated with yeast as a model organism for drug screening is the multidrug resistance (MDR) conferred by ATP-binding cassette transporters (ABC transporters) that tackle a broad spectrum of structurally and functionally different xenobiotics (Cadek et al., 2004; Rogers et al., 2001; Simon & Bedalov, 2004). The *Saccharomyces cerevisiae* genome possesses 16 genes that encode for ABC transporters (Rogers et al., 2001), which are categorized into different subclasses according to the cellular compartment occupied: ABCB (mitochondria), ABCC (vacuole), ABCD (peroxisome) and ABCG (plasma membrane) (Paumi et al., 2009). Mitochondrial ABC transporters can be located within the inner membrane (*MDL1*, *MDL2* and *ATM1*) or in the plasma membrane (STE6). The vacuole possesses six ABC transporters (*VMR1, YBT1*, *NFT1*, *YCF1, BPT1* and *YOR1*) while peroxisome has two (*PXA1* and *PXA2*). In the plasma membrane, ten ABC transporters can be found (*PDR5, PDR15, PDR10, SNQ2, PDR18, PDR12, PDR11, AUS1, YOL075c* and *ADP1*) (Paumi et al., 2009). The expression of the different ABC transporters and, subsequently the regulation of the pleotropic drug-resistance efflux pumps, is controlled by the pleiotropic drug resistance transcription factors Pdr1 and Pdr3 (Ma & Liu, 2010; Nawrocki et al., 2001). Hindering the activity of the yeast efflux plumps, for instance, through the deletion of *PDR1* and *PDR3* has shown to lead to a reduction in the efflux-mediated detoxification and a drastic increase in drug sensitivity (Rogers et al., 2001; Simon & Bedalov, 2004). Therefore, this genetic manipulation allows the circumvention of the multidrug resistance problem.

2. Study Goals

Heat shock protein 90 (Hsp90) is a highly conserved 90 kDa protein chaperone that is ubiquitously expressed in the cells of wide range of living organisms. Hsp90 establishes interactions with different client proteins through co-chaperones. One of the best studied is Cdc37, a central Hsp90 co-chaperone with a specialized role in the regulation of protein kinases (Pearl & Prodromou, 2006). Although several Hsp90 inhibitors have entered clinical trials, further clinical advancement has been hindered by their limited efficacy, inevitable heat shock response, and multiple side-effects. As an alternative, disrupting the Hsp90-Cdc37 complex rather than inhibiting all the client proteins, could avoid the limitations of current inhibitors (Serwetnyk & Blagg, 2021).

In this project we aimed to achieve two main goals: 1) Develop a yeast-based screening model for the identification of inhibitors that target the activity or disrupt protein-protein interactions of the Hsp90-Cdc37 chaperone complex and 2) through the employment of the developed screening model, search for novel Hsp90-Cdc37 inhibitory compounds that may be used in the development of improved therapeutic drugs.

3. Materials and Methods

3.1 Yeast strains and growth conditions

The *S. cerevisiae* used in this study are listed in **Table 1**. The strains were grown to exponential and post-diauxic shift (PDS) phases in Erlenmeyer flasks with a 1:5 ratio between medium volume and flask volume capacity, at 26 ˚C or 25 ˚C with agitation (140 rpm). The growth media used was either YPD (Yeast Peptone Dextrose; 2% (w/v) glucose, 2% (w/v) bacteriological peptone and 1% (w/v) yeast extract), synthetic complete (SC) drop-out medium (2% (w/v) glucose, 0.67% (w/v) yeast nitrogen base without amino acids, drop-out, and different combinations of 0.008% (w/v) methionine, 0.008% (w/v) tryptophan, 0.008% (w/v) histidine, 0.008% (w/v) uracil and 0.04% (w/v) histidine), or synthetic glucose L-proline medium (0.17% yeast nitrogenous base without ammonium sulphate, supplemented with 0.1% (w/v) proline, 2% (w/v) glucose, 0.003% (w/v) SDS and appropriate amino acids).

Table 1- Strains, genotype and sources of Saccharomyces cerevisiae used in this study.

Yeast strain	Genotype	Source
BY4741	MATa, his3Δ1, leu2Δ0, met15Δ0, ura3Δ0	EUROSCARF
cdc28^{td}	[BY4741] *cdc28-td*:KanMx4	EUROSCARF
cdc28-1	[BY4741] *cdc28-1*:KanMx4	EUROSCARF
***cka1*Δ**	[BY4741] *CKA1*Δ::KanMx4	EUROSCARF
***cka2*Δ**	[BY4741] *CKA2*Δ::KanMx4	EUROSCARF
AD1-9	MATα US50-18C *yor1Δhisg snq2Δhisg pdr5Δhisg pdr10Δhisg pdr11ΔhisG ycf1ΔhisG pdr15ΔhisG pdr1ΔhisG pdr3ΔhisG*	(Rogers et al., 2001)
AD1-9 *cdc28-1*	[AD1-9] *cdc28-1*:*URA3*	This study
AD1-9 Leu2_U	[AD1-9] *leu2*Δ::*URA3*	This study
TM141 CDC37-S14A	TM141 *cdc37*Δ::*HIS3* YCplacIII-CDC37-S14A-HA	(Hawle et al., 2007)
TM141 CDC37-S14A p50-*CDC37*	TM141 *cdc37* Δ::*HIS3* YCplacIII-CDC37-S14A-HA:URA3 YCplacIII p50-Cdc37	This study
TM141 CDC37-S14A p50	TM141 *cdc37* Δ::*HIS3* p425GPD-p50-S14A-HA:URA3	This study
AD1-9 p50-*CDC37*	[AD1-9] *leu2*Δ::*URA3* YCplacIII p50-Cdc37	This Study
AD1-9 O.E. p50	[AD1-9] *leu2*Δ::*URA3* p425GPD-p50	This Study
AD1-9 *cdc37*Δ p50-*CDC37*	[AD1-9] *cdc37*Δ:HygB YCplacIII p50-Cdc37	This Study
AD1-9 *cdc37*Δ O.E. p50	[AD1-9] *cdc37*Δ:HygB p425GPD-p50	This Study

3.2 Recombinant DNA techniques

To construct the *cdc28-1* expressing strains, *cdc28–1* sequence was amplified from BY4741 *cdc28-1* and fused to the Ura3MX6 cassette, using overlap extension polymerase chain reaction (PCR). This product was then integrated into AD1-9 strain.

To transform the AD1-9 strain with the human/chimeric *CDC37 gene,* cloned in vectors with the selection marker LEU2, the *LEU2* gene was deleted in the AD1-9 strain using URA3 amplified from pRS316 plasmid selection marker. Endogenous *CDC37* gene deletion was achieved using a *CDC37* deletion cassette amplified from pFA6a-6xGly-3xFLAG-hphMX4 plasmid (provided by Mark Hochstrasser), in order to delete 55 bases upstream of the gene, followed by hygromycin sequence, 55 bases downstream of the STOP-codon of the gene and a short sequence of complement to hygromycin gene in accordance with (Funakoshi & Hochstrasser, 2009). Confirmation of gene deletion was performed by colony PCR using one primer with homology to the selection marker and another homologous to the adjacent region of the gene mutated, as listed in **Table 2**.

The DNA cassettes (linear DNA fragments with specific marker genes used for artificial selection of transformants) used to construct the yeast mutants were amplified by PCR, using a T100™ Thermal Cycler (Bio-Rad). PCRs for cassette amplification from plasmid were performed in 50 µL reaction mixes comprised of a forward and reverse primer (both at 50 ng), 25 µL of Nzytaq II 2x Green Master Mix (NZYtech genes & enzymes), 5 ng of plasmid and ultrapure water. In colony PCR, the yeast cells were first suspended in 20 µL ultrapure water and then lysed by heating for 30 sec in the microwave at 750 W. Forward and reverse primers and NZYtaq II 2x Green Master Mix (NZYtech genes & enzymes) were added. The different primers used can be found in **Table 2**. PCR products were analysed using a nucleic acid electrophoresis at 125V for 30 min using 1% agarose gel containing GreenSafe Premium 0.04 µL/mL (NZYtech genes & enzymes) and TAE buffer (40 mM Tris, 20 mM acetic acid, 1mM EDTA). The DNA bands were observed through UV fluorescence. The purification of amplified DNA was conducted following the NZYGelpure (NZYTech) and the quantification was performed by using a NanoDrop 1000 Spectrophotometer (Thermo Fisher Scientific).

Table 2- List of primers used in the polymerase chain reaction (PCR) performed in this study.

Name	Sequence	Plasmid/ genomic	Remarks
Primers for gene-targeting			
p82 p83	5' TCCTTGACAGTCTTGACG 3' 5' GTATAGCGACCAGCATTC 3'	Genomic DNA	Confirmation of *CDC37* deletion in AD1-9
Cdc28 FD Cdc28-1 p82	5' GAAGGACCAAGTCCTCTTG 3' 5' CGTCAAGACTGTCAAGGACTAGGCTATAATGACAGTG 3'	Genomic DNA	Amplification *cdc28-1*-p82
Cdc28-1 p83R	5'GAGTTACCCATCATAATGTTGAAACTGAGTATATTGTAT TCACTATATACTGTATAGCGACCAGCATTC3'	pRS316-URA3	Fusion *cdc28-1*-URA3
Leu2_U_FW Leu2_U_RV	5' ATGTCGAAAGCTACATATAAG 3' 5' TTAGTTTTGCTGGCCGCATC 3'	pRS316	Amplification of *LEU2* deletion cassette
ClngCDC37 FW ClngCDC37 RV	5' TCTAGAGGATCCATGGTGGACTACAGCGTG 3' 5' CTCGACCTCGAGTCACACACTGACATCCTTC 3'	pET28b-p50	Human *CDC37* (p50) amplification for p426GPD cloning
CDC37hphF CDC37hphR	5' CACGATAAAAAAACTATCGAGCTATCGTACTACGGAACAA CTACATAAGTCAAAAATGGGTAAAAAGCCTGAACTC 3' 5' TAGATGCACGCTGCACCAGTAAAATAGCTACATAAATTTC TAGTCAACAGTGTC GAATTCGAGCTCGTTTAAAC 3'	pFA6a-6xGly-3xFLAG-hphMX4	Amplification of *CDC37* deletion cassette
p82 CDC28 R2	5' TCCTTGACAGTCTTGACG 3' 5' GAGTCAGATGCGAAACGG 3'	Genomic DNA	Confirmation of the integration of *cdc28-1* into AD1-9

3.3 Plasmid Construction and Amplification

In order to develop a screening yeast model expressing the human *CDC37* gene (p50), the p50 gene was cloned into a yeast multicopy vector under the control of the strong constitutive glyceraldehyde-3-phosphate dehydrogenase gene (GPD) promoter (plasmid

p425GPD). To produce the desired plasmid, the p50 gene (insert) was amplified by PCR from the pET28b-p50 (kindly provided by Dr. Chrisostomos Prodromou, UK) (**Table 2**). This PCR product and the p425GPD plasmid (isolated from *E. coli*), were double digested with the restriction enzymes B*am*HI and *Xho*I in Tango buffer 2X (Thermo Fisher Scientific) for 6 h at 37 ºC. The product was analysed by nucleic acid electrophoresis, purified and quantified. The ligation of the insert into p425GPD was performed using Rapid DNA Ligation Kit (Thermo Fisher Scientific) where 80 ng of vector (p425GPD) were incubated with the insert (1:3 molar ratio) and DNA ligase in the ligation buffer at room temperature for 16 h. The procedure was also conducted without the insert to serve as a negative control for the ligation reaction. The ligation mixture (10 µL) was used to transform 100 µL aliquot of *E. coli* through a 45 min incubation on ice, followed by 60 sec at 42 ºC and another 5 min on ice. Super Optimal broth with Catabolite repression medium (SOC-medium) (1 mL) was added and cells were incubated for 1 h at 37 ºC. Afterwards, the cells were plated in solid LB medium (1% (w/v) tryptone, 1% (w/v) NaCl, 0.5% (w/v) yeast extract) with 0.01%(v/v) ampicillin to grow overnight. An *E. coli* colony containing p425GPD-p50 was growth in liquid LB medium containing ampicillin at 37 ºC overnight. The plasmid was extracted using the NZYMiniprep (NZYTech) kit protocol and quantified using a Nanodrop 1000 Spectrophotometer before yeast transformation.

3.4 Yeast Transformation

The yeast transformations were performed following the lithium acetate/single-stranded carrier DNA/PEG protocol (Daniel Gietz & Woods, 2002) Cells (in approximately 20 mL YPD culture) were grown to exponential growth phase, centrifuged at 4200 rpm for 2 min and washed with water. The cells were resuspended in 480 µL 50% PEG (w/v), 72 µL of 1 M lithium acetate and 50 µL of 5 mg/mL single-stranded carrier DNA and equally separated into two microtubes. The proper amount of plasmid DNA/gene disruption cassette (or water, negative control) was added and tubes were incubated for 30 min at 26 ˚C and 30 min at 42 ˚C. Cells were then incubated at 26 ˚C for 4 h in YPD 2X to recover and then plated in solid YPD medium supplemented with 100 µg/ml hygromycin and incubated overnight at 26 ºC.

AD1-9 cells transformed with p425-GDP-p50 or YCplacIII-p50-CDC37 (a gift from Dr. Mehdi Mollapour, USA) were incubated at room temperature for 30 min, and then at

42 ˚C for 20 min before being washed and plated in SC medium lacking leucine. For transformation of TM141 cells, containing the temperature-sensitive Cdc37-S14A mutation, with p425-GPD-p50 or YCplacIII-p50-CDC37, the heat-shock step was omitted and replaced for a room temperature incubation for 3 h, plated in YPD medium and incubated overnight directly at 37 ºC to assess for growth complementation.

3.5 Inhibition Halo Assay

A small volume of saturated starter culture (for an optical density (O.D.) of 4, 70 µL of AD1-9 strain and 175 µL of AD1-9 *cdc28-1* strain) was mixed in the tube containing 3 mL of YPD with 0.5% agar (kept in a 50°C water bath) and then poured in a pre-warmed plate containing YPD solid media (2% agar) in order to obtain a uniform cell lawn. Paper disks containing 4 µL of the different compounds tested or control (solvent, DMSO) were placed on the solid cell/agar lawn. The compounds tested were the commercial Hsp90 inhibitor 17-AAG (2.5 mg/mL) and geldanamycin (5 mg/mL), the yeast protein synthesis inhibitors cycloheximide (0.025 mg/mL) and geneticin (4 mg/mL), the Hsp90-Cdc37 interface inhibitors platycodin D (5 mg/mL) and elaiophylin (5 mg/mL), and a collection of *in-house* compounds (5 mg/mL), (in collaboration with E. Sousa, CIIMAR). The plates were incubated at 26 °C for 1-2 days.

3.6 Western Blot

Cells were grown to early exponential phases in SC containing DMSO, 17-AAG (1 µg/mL) or the hit compounds xanthone 3, 5, 17 (all at 10 µg/mL), 6 (15 µg/mL) and 9 (5 µg/mL), washed with water, pelleted, and resuspended in Laemmli sample buffer 2X (4% (w/v) SDS, 20% (v/v) glycerol, 0.004% (w/v) bromophenol blue and 0.125M Tris HCl, pH 6.8). The samples were heated at 95 ˚C for five min, vortexed for three min in the presence of zirconia beads and then centrifuged for 2 min at 13 400 rpm to remove debris. The supernatant containing the soluble proteins was collected.

The protein samples were separated by SDS-polyacrylamide gel electrophoresis (SDS-PAGE) in a 12% polyacrylamide gel at 70-90 V and then transferred to a nitrocellulose membrane using Tris-glycine transfer buffer (59.9 mM Tris, 48.8 mM glycine, 1.62 mM SDS) with the addition of 20% (v/v) methanol for a semi-dry transfer

system for 1 h at 45 mA. The membrane was then stained with Ponceau S (0.5% (w/v) Ponceau S, 5% (v/v) acetic acid) and washed with Tris-buffered saline (TBS- 19.8 mM Tris, 150.6 mM NaCl, pH 7.6). Afterwards, the membrane was blocked for 1 h at room temperature using dry powder milk (5% w/v) in TBS with 0.05% (v/v) Tween-20 (TTBS) (20 mM Tris, 140 mM NaCl, 0.05% (v/v) Tween-20, pH 7.6). The membrane was incubated overnight at 4 ˚C with primary antibodies, mouse anti-CDC28 (Santa Cruz Biotechnology 1:150) and mouse anti-PGK (Invitrogen 1:40000), or at room temperature for 45 min with primary antibody rabbit anti-Hexokinase (Hxk) (Rockland 1:100000) in dry powder milk (5% w/v) in TTBS with 0.05% (v/v) Tween-20. The membranes were then washed briefly with TBS followed by two 5 min and one 10 min washes with TTBS. Afterwards the membrane was incubated at room temperature for 1-2 h with peroxidase-linked secondary antibodies, anti-mouse (Invitrogen 1:5000) for Cdc28 detection, anti-mouse (Invitrogen 1:7000) for PGK1 and anti-rabbit (Sigma-Aldrich 1:7000) for Hxk. The membranes were once again washed two times for 5 min and once for 10 min with TTBS and one more time for 5 min with TBS. The immunodetection was achieved by chemiluminescence using WesternBright™ ECL detection Kit (Advansta) and exposure to a LucentBlue X-ray film (Advansta). The film was scanned on a Molecular Imager GS800 and protein band intensities were quantified using Quantity One 1-D Analysis Software version 4.6 (Bio-Rad).

3.7 *E. coli* growth and plasmid purification

E. coli carrying the desired plasmids (YCplacIIIp50CDC37, pET28Bp50-HIS6, YCplacIIICDC37-S14A.S17A-HA and p425GPD-p50) were grown overnight at 37 ˚C in liquid lysogeny broth medium (LB) supplemented with 0.01%(v/v) ampicillin. The extraction and purification of the plasmid DNA was performed using NZYMiniprep (NZYTech).

3.8 Statistical analysis

The statistical analysis was performed using GraphPad Prism software (version 8.3.0) and values were compared using the two-tailed t-test ($p<0.05$) and the one-way ANOVA ($p<0.05$). The results are displayed containing the mean and standard error of the mean (SEM) or standard deviation (SD) for three to four independent experiments.

4. Results and Discussion

4.1 The *cdc28-1* mutant strain is sensitive to Hsp90 inhibition in liquid cultures

To develop a yeast model to screen for inhibitors of the Hsp90-Cdc37 chaperone complex, we decided to use as a readout the increased sensitivity of yeast strains associated with loss of Hsp90-Cdc37 function when compared to wild-type strains in order to distinguish the effect of compounds that specifically target the chaperone complex from the ones that have an Hsp90-independent inhibitory effect in cell growth. As previously stated, the Hsp90-Cdc37 chaperone complex is regulated through phosphorylation by the CK2α kinase. This regulation is also conserved in yeast (Bandhakavi et al., 2003) and, therefore, compromising CKII leads to a lower chaperone complex activation and consequently an increased sensitivity towards chaperone inhibition. Two strains lacking the casein kinase catalytic subunit 1 or 2, *cka1*Δ and *cka2*Δ respectively, were selected. Increased Hsp90-Cdc37 dependency, and hence, higher sensitivity to Hsp90 inhibition, can be induced through the mutation of essential client proteins. Cdc28 is the catalytic subunit of the main cell cycle cyclin-dependent kinase in budding yeast (Kitazono et al., 2003). Through the formation of the Hsp90-Cdc37 chaperone complex, Hsp90 interacts with Cdc28 conferring the kinase the necessary stability for its activity (Farrell & Morgan, 2000). Two strains containing a mutation in the Cdc28 gene were used: the *cdc28*^{td}, characterized by the presence of a degron motif that renders the protein temperature sensitive, and the *cdc28-1* temperature-sensitive point mutant. The presence of a tag or a structural alteration are known to depend more heavily on Hsp90 activity, therefore enhance the effect induced by chaperone inhibition.

The four different mutant strains (*cdc28*^{td}, *cdc28-1, cka1*Δ *and cka2*Δ), along with the wild-type BY4741 strain that served as a control, were grown to stationary phase in minimal L-proline medium. The addition of 0.003% SDS to this medium improves the cell permeability to drugs through the transient opening of the cell wall/membrane (Liu et al., 2007). In order to assess the effect of Hsp90 inhibition on cell growth, the known NTD inhibitor 17-N-allyloamino-17-demethoxygeldanamycin (17-AAG), or the solvent DMSO, were added to the cultures and overnight growth was monitored by measuring $O.D._{640nm}$. We found that 17-AAG inhibited the growth of all strains (**Fig. 4**). This inhibition, however,

was higher in the *cdc28-1* strain (42% less growth) compared to the wt strain (15% inhibition) and the *cdc28-1* mutant was selected to further implement the yeast screening model. Though *cka*Δ *mutants* in yeast were previously reported as GDA sensitive (Bandhakavi et al., 2003), only *cka2*Δ exhibited a mild increase in in 17-AAG (GDA derived) sensitivity.

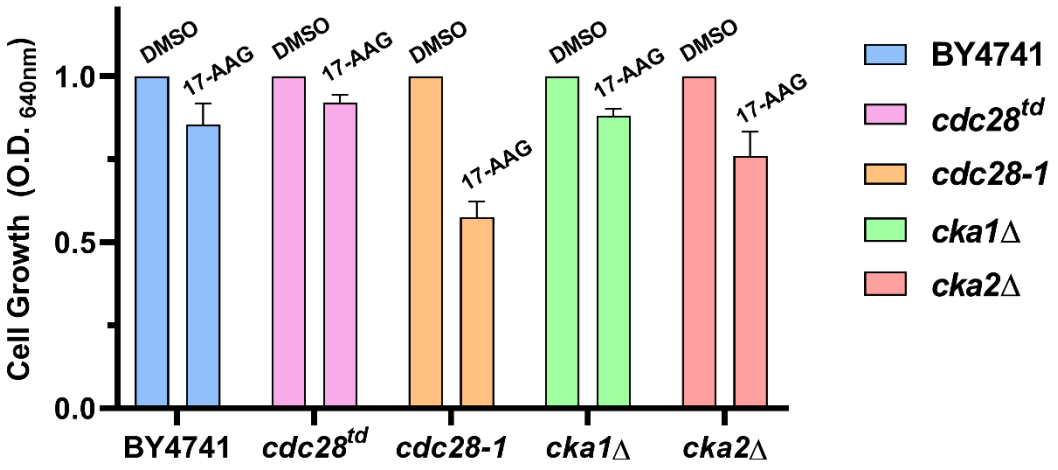

Figure 4- The *cdc28-1* mutant strain displays enhanced sensitivity to Hsp90 inhibitor 17-AAG. The growth of mutant yeast strains with higher Hsp90-Cdc37 chaperone complex dependency, *cdc28^{td} cdc28-1*, *cka1*Δ and *cka2*Δ was assayed in comparison with wild-type strain BY4741. The cells from different strains were grown to stationary phase in high glucose L-proline medium and were either treated with the negative control DMSO or the Hsp90 inhibitor 17-AAG Values are the mean ± SD (n=2).

4.2 Manipulation of the multidrug resistance factors improves sensitivity to Hsp90 inhibitors

The drug discovery process requires the study of a wide range of compounds and, testing different compound concentrations is required to fully understand its effect in comparison to already established compounds. The simplest method is growth-inhibition assay. We opted for a halo inhibition assay, in which a small amount of compound is added to a paper filter, and growth inhibition is detected by the formation of a “halo” with no growth. The advantage of this method is that, in one simple experiment, it allows

numerous compounds to be tested across a large range of concentrations due to diffusion of the drugs in the growth medium, improving the sensitivity of the screen drastically. However, despite the wt and *cdc28-1* strain sensitivity to 17-AAG in liquid media, when we tried to adapt this assay to solid media, no inhibition halo was formed using the wt strain (**Fig. 5A**) or the more sensitive *cdc28-1* strain (not shown).

The multidrug resistance exhibited by *S. cerevisiae* represents a major hurdle in the development of screening protocols when using the yeast model. This resistance to a broad range of compounds is mounted by the ABC transporters that can be located in several sub-cellular compartments and is regulated by the pleiotropic drug resistance genes *PDR1* and *PDR3*. Here, it was postulated that this drug resistance was the leading factor in the inability demonstrated by known Hsp90 inhibitors to cause growth arrest. The AD1-9 strain (represented in **Fig. 5C**) is characterised by the deletion of five ABC-transporters located in the cell membrane, namely *PDR5*, *PDR15*, *PDR10*, *SNQ2*, *PDR11*, and two located in the vacuole, *YCF1* and *YOR1*. Moreover, The *PDR1* and *PDR3* transcription factors that promote ABC-transporter expression have also been deleted (Rogers et al., 2001). The deletion of the regulatory genes as wells as the seven ABC genes produced a yeast strain that possesses highly increased sensitivity to a myriad of compounds, including the Hsp90 inhibitor 17-AAG (Millson et al., 2010; Rogers et al., 2001).

Inhibition halo assays were then performed using the AD1-9 strain in YPD solid medium (**Fig. 5B**). The yeast protein synthesis inhibitors geneticin (G418) and cycloheximide (CHX) and the Hsp90 inhibitors geldanamycin and 17-AAG were analysed. DMSO was used as a solvent control. In this drug-sensitive strain, the compounds, except GDA, induced growth arrest visible by the formation of a growth inhibition halo. The lack of growth arrest caused by GDA is most likely associated with the compound reduced aqueous solubility (Ge et al., 2006).

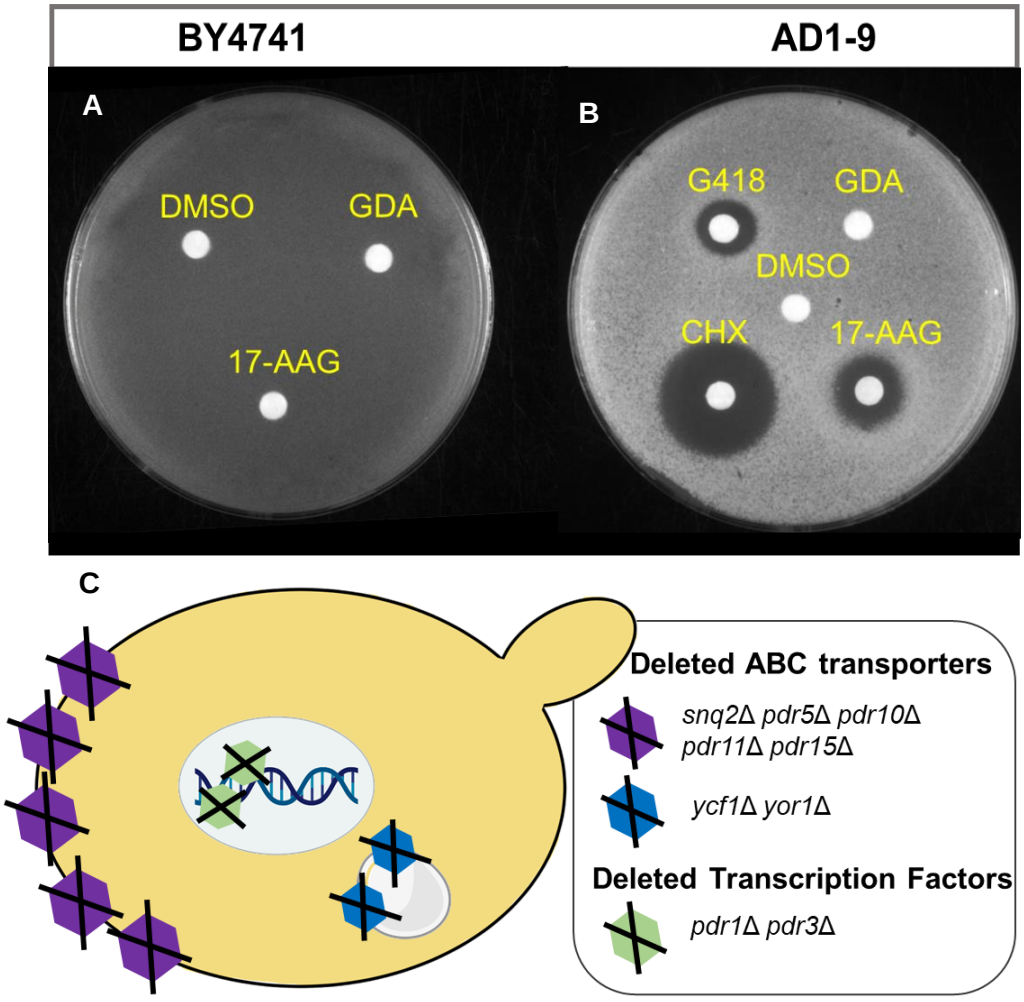

Figure 5- AD1-9 mutant showed enhanced sensitivity to compound induced growth arrest compared to wild-type BY4741. Growth arrest (inhibition halos) assay was tested in both the BY4741 and AD1-9 strains grown to stationary phase in solid minimal L-proline media and YPD medium respectively. **A-** The effect of known Hsp90 inhibitors geldanamycin (GDA) and 17-N-allyloamino-17-demethoxygeldanamycin (17-AAG) at 5 and 2.5 mg/mL respectively was assayed in the wild type BY4741 strain. DMSO was the solvent control. **B-** The effect of specific Hsp90 inhibitors GDA, 17-AAG (as before) and protein synthesis inhibitors cycloheximide (CHX) at 0,025 mg/mL and geneticin (G418) at 4 mg/mL was assayed in the drug hypersensitive AD1-9 mutant strain. DMSO was the solvent control. **C-** Representation of the deleted ABC transporters and Transcription factors responsible for AD1-9 strain drug sensitivity.

4.3 Using *cdc28-1* mutation to establish a screening model in AD1-9 for Hsp90-Cdc37 inhibitors

Using the AD1-9 strain as a parental strain to develop the screening model, the *cdc28-1* mutation was genomically integrated replacing the endogenous *CDC28,* to have a bias toward the Hsp90-Cdc37 inhibition. The halo inhibition assay was repeated using the same compounds, namely the fungicides geneticin (G418) and cycloheximide (CHX) tested as controls for Hsp90-Cdc37-independent growth inhibitions, and geldanamycin and 17-AAG as positive controls for Hsp90 inhibition. As in liquid minimal L-proline media, we found 17-AAG induced growth inhibition. Notably, compounds that inhibit Hsp90-Cdc37 induced a larger halo of growth inhibition in *cdc28-1* versus wt cells (**Fig. 6A** and **B**), while the unspecific yeast growth inhibitors (G418 and CHX) resulted in similar size halos in both strains. The average size difference between the halos formed in both strains by CHX, the stronger broad effect inhibitor, was established as a cut-off point in the screening of Hsp90-Cdc37 inhibitors. The growth inhibition induced through general toxicity or other Hsp90-Cdc37 independent mechanisms are expected to lead to halo size differences comparable to the limit established by CHX. The growth arrest induced by 17-AAG in the AD1-9 *cdc28-1* strain was nearly 1.5-fold the effect registered in the AD1-9 strain. This effect is less evident with GDA since, as referred before, it induces a very low growth inhibition. In sum, using the AD1-9 *cdc28-1* strain we were able to establish a Hsp90-Cdc37-selective sensitive assay. This model will allow for a simple and fast screening for Hsp90, Cdc37 and Hsp90-Cdc37 interaction inhibitors. An added advantage for using the AD1-9 strain is the ability to use rich YPD medium, instead of minimal L-proline, a more expensive medium.

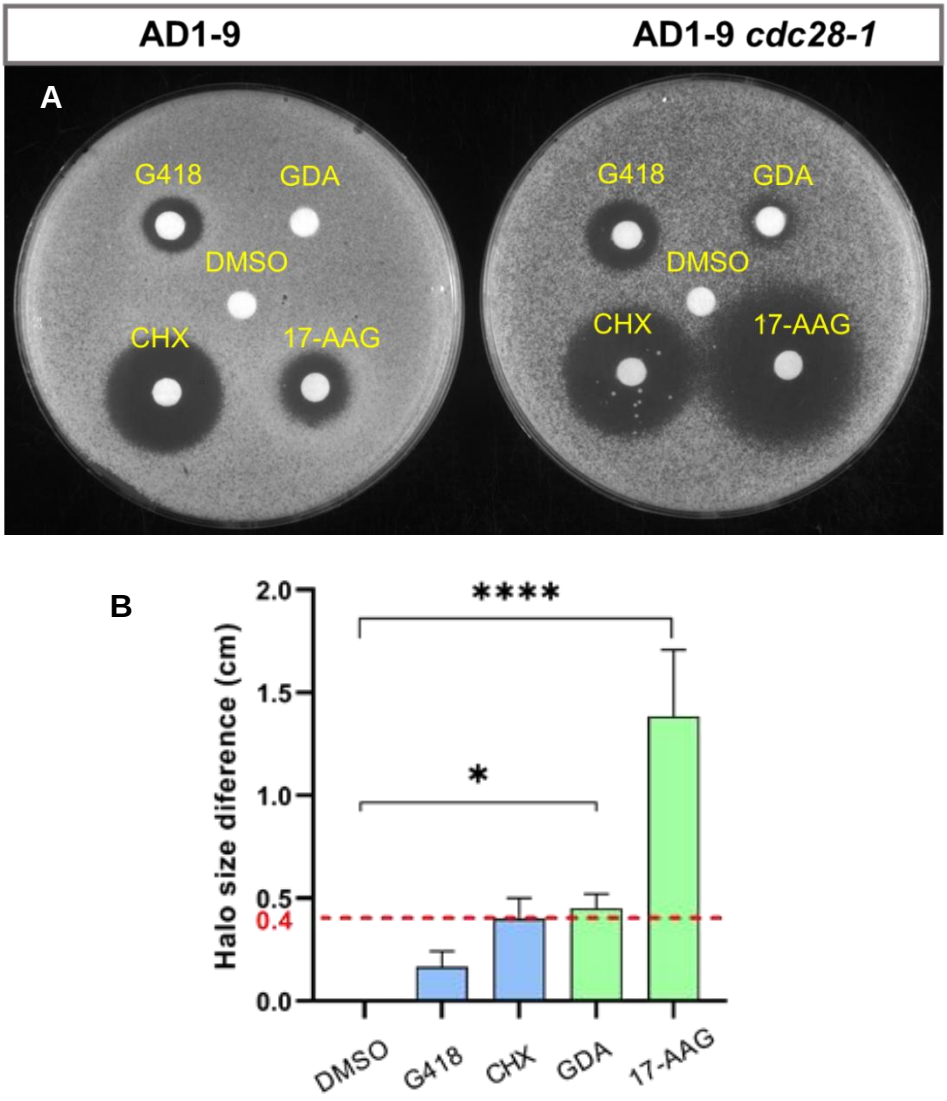

Figure 6- Compound response phenotypes of AD1-9 and AD1-9 *cdc28-1* strains. Growth arrest (inhibition halos) was induced by different compounds in both the AD1-9 and AD1-9 *cdc28-1* mutant strains grown to stationary phase in solid YPD medium. **A-** The effect of broad protein synthesis inhibitors cycloheximide (CHX) at 0.025 mg/mL and geneticin (G418) at 4 mg/mL as well as known NTD Hsp90 inhibitors geldanamycin (GDA) at 5 mg/mL and 17-N-allyloamino-17-demethoxygeldanamycin (17-AAG) at 2.5 mg/mL was assessed in AD1-9 and AD1-9 *cdc28-1* strains. DMSO was used as a solvent control. A representative image is shown. **B-** Graphical representation of the average halo difference formed in the AD1-9 and the AD1-9 *cdc28-1* strains (n=2-3). The non-specific inhibitors are represented in blue while the Hsp90 specific inhibitors are represented in green. The dotted red line represents the cut-off point of 0.4 determined by the effect of the non-specific inhibitors. The values shown are the mean ± SEM with $p<0.05$, t-student´s test.

4.4 Potential Hsp90-Cdc37 inhibitors were identified using the yeast halo-assay screening model

Using the implemented yeast halo-assay screening model, we tested 79 pre-selected compounds from 4 in-house libraries of xanthones, xanthenes, chalcones, homoisoflavonoids and diarylpentanoids (**Table 3**). These compounds were provided in a partnership with the Interdisciplinary Centre of Marine and Environmental Research (CIIMAR). The average halo size difference between the AD1-9 strain and the AD1-9 *cdc28-1* strain was below the defined cut-off threshold for all but for eight compounds (**Table 3** and **Fig. 7**). From these eight compounds only six (xanthones 3, 5, 6, 7, 9, 17) were selected for further studies, since two of the compounds showed very mild effects. Xanthones 5 and 17 showed the most promising effects.

Table 3- Compounds used in the yeast halo-assay screening for Hsp90-Cdc37 inhibitors. Compounds exhibiting potential Hsp90-Cdc37 inhibitory effect are highlighted in grey.

	Compound Number	Compound Code	Molecular Mass (g/mol)	Specific Inhibitory Effect
Xanthones (E. Sousa)	**1**	**X**	196.21	Yes
	2	**1HX**	212.20	No
	3	**2HX**	212.20	Yes
	4	**3HX**	212.20	No
	5	**4HX**	212.20	Yes
	6	**1METOXIX**	226.23	Yes
	7	**2METOXIX**	226.23	Yes
	8	**4METOXIX**	226.23	No
	9	**12DIHIDROXIX**	228.20	Yes
	10	**23DIHIDROXIX**	228.20	No
	11	**34DIHIDROXIX**	228.20	No
	12	**17DIHIDROXIX**	228.20	No
	13	**36DIHIDROXIX**	228.20	No
	14	**12DIMETOXIS**	256.26	No
	15	**23DIMETOXIS**	256.26	No
	16	**34DIMETOXIS**	256.26	No
	17	**4HIDROXI3METOXIX**	242.23	Yes
	18	**13DIHIDROXI2METOXIX**	258.23	No
	19	**1F34DIHIDROXIX**	256.21	No
	20	**1F346TRIMETOXIX**	284.27	No
	21	**1F4HIDROXI3METOXIX**	314.29	No
	22	**1F4HIDROXI3METOXIX**	270.24	No

	23	**1E346TRIMETOXIX**	344.32	No
	24	**2F3HIDROXI4METOXIX**	270.24	No
	25	**1M34DIMETOXIX**	242.23	No
	26	**2CL1M 34DIMETOXIX**	270.28	No
	27	**1M346TRIMETOXIX**	304.73	No
	28	**1DIBRM34DIMETOXIX**	300.31	Yes
	29	**1DIBRM346TRIMETOXIX**	428.08	No
	30	**1DBRM346TRIMETOXIX**	458.10	No
	31	**18DIHIDROXI36DIMETILX**	256.26	No
	32	**36DICLX**	265.09	No
	33	**36-DMEX**	312.28	No
	34	**36.DOTfX**	492.32	No
	35	**SZ 11.1**	362.47	No
	36	**SZ 12.1**	415.38	No
	37	**SZ 16**	364.45	No
	38	**DR 101.2**	488.59	No
	39	**XF.HCL**	443.90	No
	40	**AX13.HCL**	420.93	No
	41	**XA20**	416.48	No
Xanthenes (M. Maia)	**42**	**MM81** (C16H17NO2)	255.32	No
	43	**MM85** (C21H19NO2)	317.39	No
	44	**MM88** (C23H21NO2)	343.43	No
	45	**MM90** (C18H21NO2)	283.37	No
	46	**MM91** (C17H17NO2)	267.33	No
	47	**MM92** (C17H13F6NO2)	377.29	No
	48	**MM94** (C21H19FN2O)	334.39	No
	49	**MM95** (C17H18N2O)	266.34	No
	50	**MM96** (C16H15N5O)	293.33	No
	51	**MM97** (C19H17N3O)	303.37	No
	52	**MM98** (C19H18N2O2)	306.37	No
	53	**MM99** (C19H22N2O)	294.4	No
	54	**MM103** (C15H12BrNO4)	350.17	No
Chalcones (D. Pereira e H. Cidade)	**55**	**DPC 34 Click**	711.68	No
	56	**DPC 345 Click**	741.70	No
	57	**DPC 34 Click2**	755.73	No
	58	**RF 345 Click 2**	785.76	No
	59	**DP34 CC4 MF**	529.55	No
	60	**RF 34 Click 1**	559.58	No
	61	**DP 34 CCO H**	439.47	No
	62	**RF 345 Click 3**	469.49	No
Homoisoflavonoids (H. Cidade)	**63**	**C1-C4**	254.05	No
	64	**CiM45-C4**	314.07	No
	65	**CiM56-C4**	314.07	No
	66	**CT-C4**	268.07	No
	67	**CC-C4**	270.04	No
	68	**CTC-C4**	286.02	No

	69	**CTM67-C4**	328.09	No
Diarylpentanoids (H. Cidade)	**70**	**BP-C4**	344.04	No
	71	**BA-C4**	302.03	No
	72	**BPE-C4**	328.04	No
	73	**BHE-C4**	342.06	No
	74	**BTP-C4**	360.01	No
	75	**BP-M345**	456.18	No
	76	**BA-M345**	414.17	No
	77	**BPE-M345**	440.18	No
	78	**BHE-M345**	454.20	No
	79	**BTP-M345**	472.16	No

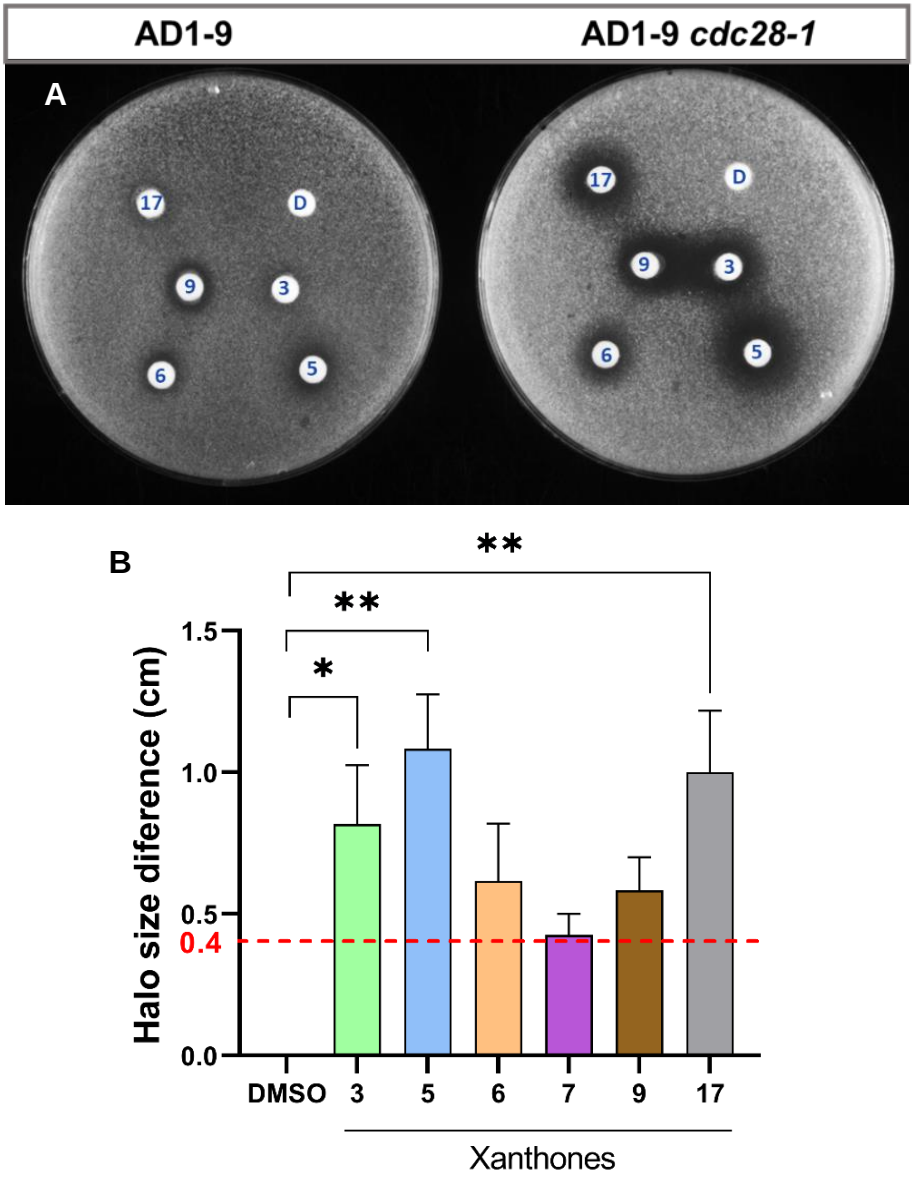

Figure 7- Screening of xanthones using the AD1-9 and AD1-9 *cdc28-1* strains. Growth inhibition (halo formation) induced during the screening different unknown xanthones in both the AD1-9 (Left) and AD1-9 *cdc28-1* (Right) mutant strains grown to stationary phase in solid YPD medium. **A-** Inhibition halos induced by the more promising screened xanthones (3, 5, 6, 9 17) all at 5 mg/mL in the AD1-9 control strain and the AD1-9 *cdc28-1* sensitive strain. DMSO (D) was used as solvent control. **B-** Graphical representation of the halo difference formed by the xanthones 3 (green), 5 (blue), 6 (orange) 7 (purple), 9 (brown) and 17 (grey) in the AD1-9 and the AD1-9 *cdc28-1* strains. The dotted red line represents the minimum halo difference value considered to categorize a compound as a specific inhibitor. The values shown are the mean ± SEM (n=3).

To compare the potency of our hit compounds with that of known Hsp90-Cdc37 direct protein-protein interface inhibitors, the inhibitory effect of platycodin D and elaiophylin

were assessed (**Fig. 8**). However, the results showed no growth arrest by either of the PPI inhibitors tested.

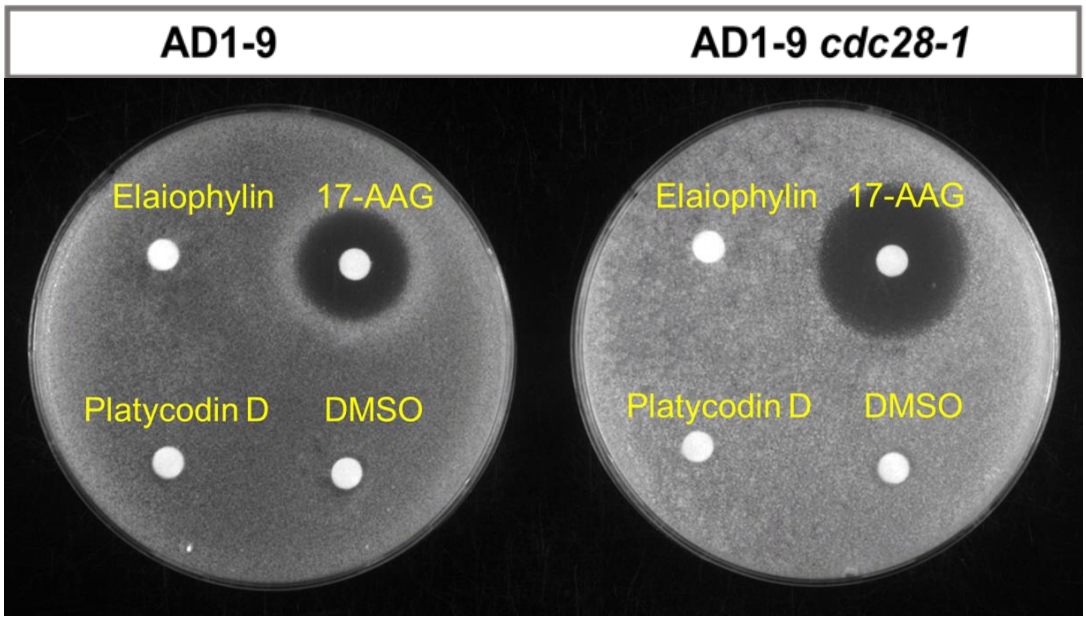

Figure 8- Screening of known PPI inhibitors using the AD1-9 and AD1-9 *cdc28*-1 strains. Both strains were grown to stationary phase in solid YPD medium**.** Growth arrest (inhibition halos) induced by the known Hsp90 inhibitor 17-N-allyloamino-17-demethoxygeldanamycin at 2.5 mg/mL and the surface PPI inhibitors platycodin D and elaiophylin, both at 5 mg/mL. DMSO was used as a negative control.

4.5 Development of "humanized" Cdc37 yeast models for screening of Hsp90-Cdc37 inhibitors

The apparent lack of sensitivity towards Hsp90-Cdc37 chaperone PPI inhibitors platycodin D and elaiophylin suggests that the current screening model may not recapitulate the interactions between Hsp90 and human Cdc37 (p50). Yeast Cdc37 is a protein of 506 amino acids while the human Cdc37 contains 378 residues and is only 19% identical to yeast Cdc37 (MacLean & Picard, 2003). This high degree of divergence may explain the lack of effect of the known human Cdc37 inhibitors for the yeast Cdc37 protein. We sought to improve our screening model by replacing the yeast *CDC37* gene with the human *CDC37* gene or p50. It is known that human p50 does not functionally substitute for yeast Cdc37 due to an essential function of the

yeast Cdc37 C-terminal domain that is not present in human Cdc37. To overcome this problem, some authors have constructed chimeras, containing the human p50 N-terminal domain, and the yeast Cdc37 middle and C-terminal (Mollapour et al., 2011). However, although the expression of human Cdc37 does not replace for *S. cerevisiae* or *S. pombe* Cdc37, its overexpression can complement *S. pombe* Cdc37 (Turnbull et al., 2005). As such, we decided to test the two approaches: i) replacing the yeast Cdc37 for a p50/Cdc37 chimera or ii) replacing the yeast Cdc37 for the overexpression of the full-length p50.

To replace the yeast *CDC37* by a chimeric human-yeast fusion, we used a construction containing the N-terminal 149 bp of the human gene fused with the middle and C-terminal 289 bp of the yeast *CDC37* under the control of the endogenous yeast *CDC37* promoter. The chimeric protein produced has a homology to the human protein of approximately 60% identity, while the yeast protein only has 19% homology. To implement the second approach, the human *CDC37* gene (p50) gene was amplified and cloned in the p425GPD plasmid, downstream the strong GPD constitutive promoter.

Since *CDC37* is an essential gene, before deleting *CDC37* in the AD1-9 strain, we first assessed if both the chimera and the overexpression of p50 were able to functionally substitute the yeast Cdc37. For that, we transformed with these vectors a strain carrying a temperature sensitive loss of function mutation in Cdc37 (Cdc37-S14A) that is unable to grow at temperatures higher or equal to 37 ºC. The strains temperature sensitive strain allows for the selection of transformants using YPD medium at 37 ºC, without the requirement of a selection mark. We found that both the chimeric gene and *CDC37* overexpression were able to generate viable colonies in the Cdc37-S14A strain at the restrictive temperature, while none grew in the control plate (**Fig. 9).** Although the p425-GPD-p50 was not so efficient in generating colonies, because the chimera does not contain the full human protein, we decided to further test both constructions.

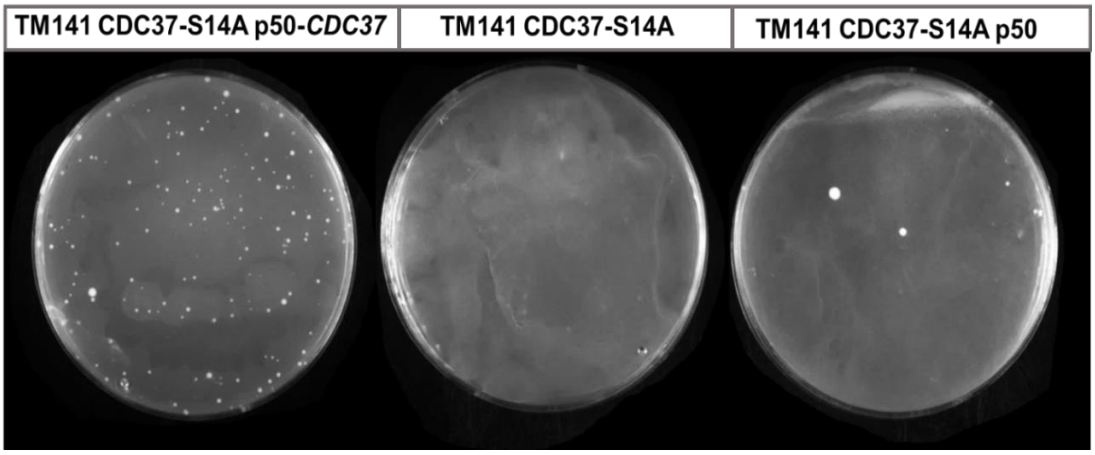

Figure 9- Cell growth in strains expressing the chimeric or human *CDC37* gene. TM41 CDC37-S14A cells untransformed (centre) or transformed with p50-*CDC37* (left) or human p50 (right) were grown at 37 ºC in YPD medium to assess mutant viability.

Since both YCplacIII and p425 plasmids have *LEU2* as a selection marker, and this gene is expressed in the AD1-9 strain, the deletion of *LEU2* gene was the first step in the development of the Cdc37 humanized models. After *LEU2* deletion in AD1-9, the strains were transformed with either YCplacIII-p50-Cdc37 chimera or the p425-GPD-p50. The transformants were deleted for the endogenous *CDC37* (**Fig. 10**). The developed mutant expressing the full-length p50 gene provides a more accurate representation of the Hsp90-Cdc37 interaction in human cells.

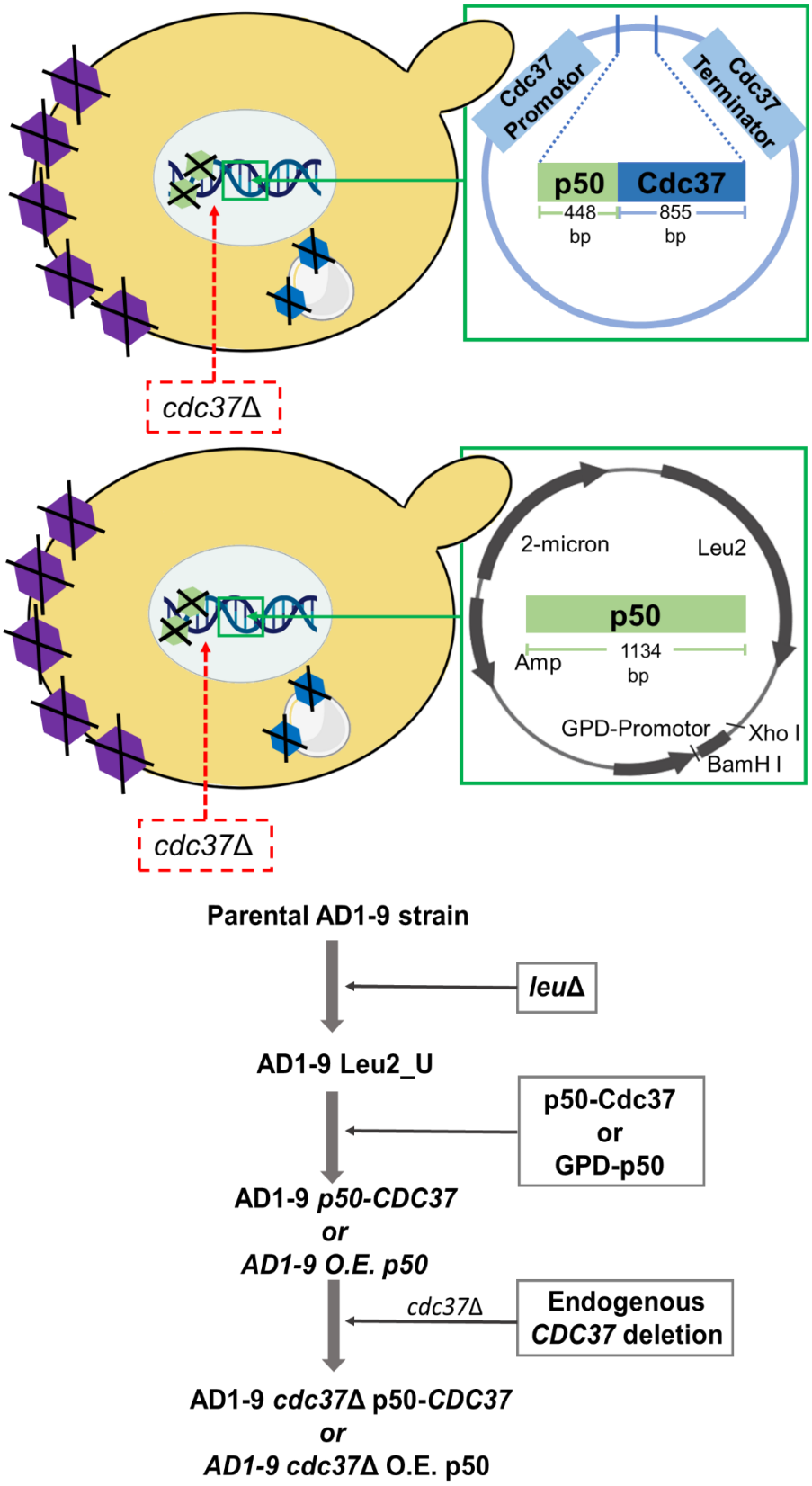

Figure 10- Development of mutant AD1-9 strains expressing the chimeric human-yeast *CDC37* gene or overexpressing the human p50 gene. Representation of the AD1-9 *cdc37Δ* p50-*CDC37* (Top) and the AD1-9 *cdc37Δ* O.E. p50 (Bottom) strains developed as well as the steps performed to develop both strains from the parental AD1-9 strain.

4.5.1 Hsp90-Cdc37 selective PPI inhibitors do not inhibit yeast growth

The effect of the specific PPI inhibitors platycodin D and elaiophylin was assessed in the developed "humanized" Cdc37 models. In strains expressing the Cdc37-p50 chimera or overexpressing (O.E.) p50 in a null background for yeast Cdc37, platycodin D and elaiophylin failed to produce an inhibition halo (**Fig. 11**). Assuming that the tested PPI inhibitors are in fact efficient and specific Hsp90-Cdc37 inhibitors, this suggests the implemented models are still not efficient for the screening of this type of compounds. In future work it will be important to integrate *cdc28-1* mutation in the "Humanized" models to increase the sensitivity of the screening. If we still do not detect any growth inhibition, the construction of a fully humanized model for the Hs90-Cdc37 pathway should be evaluated. Although Hsp90 and the yeast orthologs, Hsc82 and Hsp82, share a high sequence identity (60%), potential differences in the Hsp90-Cdc37 interaction may cause lack of disruption of this interaction by inhibitors of the corresponding human interaction.

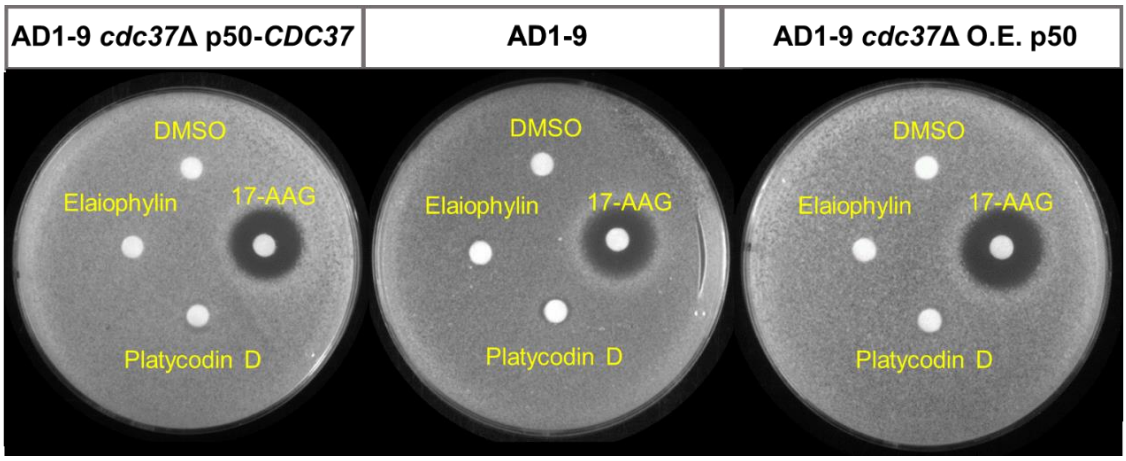

Figure 11- Screening of known Hsp90-Cdc37 PPI inhibitors using the AD1-9, AD1-9 *cdc37Δ* p50-*CDC37* and AD1-9 *cdc37Δ* O.E. p50 strains. All strains were grown to stationary phase in solid YPD medium. Growth arrest (inhibition halos) induced by the known Hsp90 inhibitor 17-AAG at 2.5 mg/mL and the surface PPI inhibitors platycodin D and elaiophylin, both at 5 mg/mL. DMSO was used as a solvent control.

4.6 Hsp90-Cdc37 target Cdc28 is destabilized upon chaperone inhibition

Treatment of cells with either Hsp90 or Hsp90-Cdc37 inhibitors leads to the unfolding and subsequent degradation of proteins that rely in the chaperone/chaperone complex to achieve correct folding. The fact that Hsp90-Cdc37 PPI inhibitors had no effect on our yeast model (humanized for Cdc37 or not), but the general Hsp90 inhibitors were effective, we questioned if the hit xanthones are targeting Hsp90 and not the Hsp90-Cdc37 interaction. Several authors use the destabilization of Hsp90 substrates including the kinase homologues of Cdc28, as molecular markers of Hsp90 inhibition in human cell lines (Buolamwini & Adjei, 2003). To determine if inhibitors are targeting Hsp90 or Cdc37/PPI inhibitors, the levels of Cdc37-dependent and Cdc37-independent protein targets were assessed. Cdc37 independent targets, i.e., proteins that depend on Hsp90 binding to co-chaperones other than Cdc37, are expected to be destabilized through the action of Hsp90 inhibitors such as 17-AAG. Hexokinase (Hxk) was reported to physically interact both with Hsp82 and Hsc82, suggesting it is an Hsp90 target (Girstmair et al., 2019). Since Hxk is not a protein kinase and no physically interaction with Cdc37 was reported, it is predicted to be a Cdc37-independent substrate and as such, it was evaluated as a potential marker for Hsp90 inhibition in a Cdc37-independent form.

Cdc28 was used as a marker of Cdc37-dependent inhibition. The destabilization of protein targets that rely on the Hsp90-Cdc37 chaperone complex such as Cdc28 without the destabilization of Cdc37-independent targets, may indicate a specific inhibition of Hsp90-Cdc37 PPI or Cdc37. Given the similar inhibitory phenotype observed in the AD1-9 and the AD1-9 humanized Cdc37 strains when treated with 17-AAG, the AD1-9 strain was selected. Since the *cdc28-1* mutant is more prone to unfolding and degradation, we first compared the suitability of using AD1-9 or the AD1-9 *cdc28-1* strain. Cells from both strains were grown in liquid YPD media and treated with either DMSO as a negative control, or with the Hsp90 inhibitor 17-AAG (1µg/mL) until they reached early exponential (log) phase. The concentration of 17-AAG was reduced comparing to the solid media assays in order to obtain 50% growth inhibition for all the tested compounds. Afterward, the cells were collected, and a western blot was performed to analyse Cdc28 and Hexokinase (Hxk) levels. Since a large amount of proteins are Hsp90 targets (627 putative substrates representing approximately 10% of the yeast proteome) (Zhao et al.,

2005), and many remain unidentified, in addition to use single proteins as a loading control, the mean between Phosphoglycerate Kinase 1 (Pgk1) and an unspecific band from Hxk detection was used as a loading control in order to minimize the potential direct or indirect effects of Hsp90 inhibition.

The membranes were stained with Ponceau S in order to assess the total protein concentrations in each sample and confirm the selected loading controls as good representatives of total protein differences (**Fig. 12A**). In both AD1-9 and AD1-9 *cdc28-1,* treatment with 17-AAG caused a strong decrease in Cdc28 levels compared with the control DMSO (**Fig. 12A** and **12B**). These results show that in yeast Cdc28 levels are also destabilized upon Hsp90 inhibition. In AD1-9 *cdc28-1* cells, the levels of Cdc28 were already low and further decreased upon 17-AAG treatment to below the detection limit. Since a clearer difference in Cdc28 levels between treated and untreated cells was obtained for AD1-9 carrying wt Cdc28, we selected this strain to test the effect of the hit xanthones in the Cdc28 levels. The protein levels of Hxk were also reduced in both strains when treated with 17-AAG comparing to DMSO-treated control cells (**Fig. 12A** and **12C**). This result suggests that the destabilization of Hxk can be used as a marker of Hsp90 inhibition.

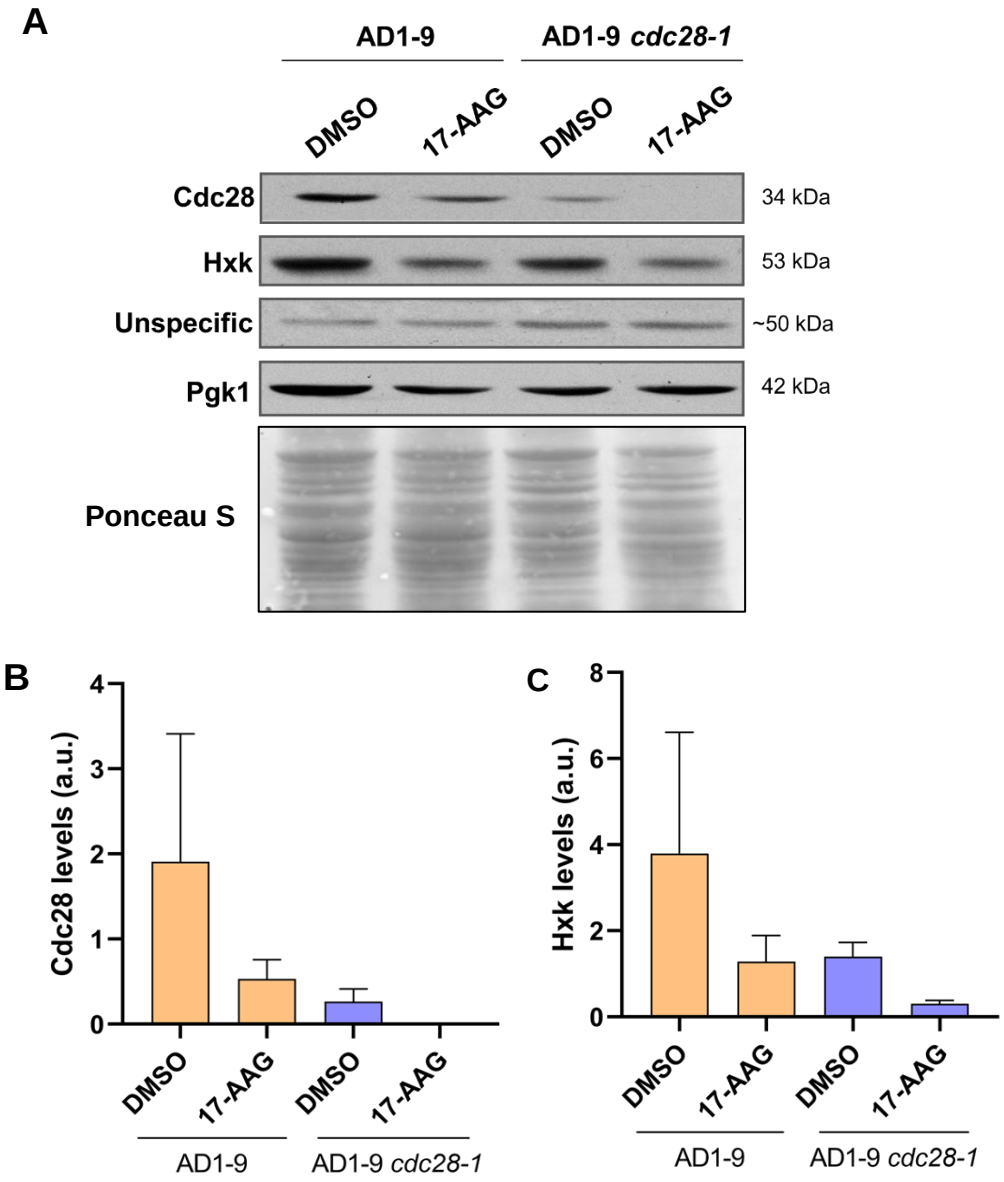

Figure 12- Cdc28 and Hxk are destabilized in both AD1-9 and AD1-9 *cdc28-1* strains. A- *S. cerevisiae* AD1-9 cells were grown to early exponential (log) phase in liquid YPD medium and treated with either the solvent DMSO (negative control) or Hsp90 inhibitor 17-AAG (1 µg/mL). Cdc28 and Hxk levels were assessed by western blotting. The average between Pgk1 and an unspecific Hxk band was used as loading control. Ponceau S staining reflects total protein content the samples. **B-** Quantification of Cdc28 levels normalized to loading in both AD1-9 (orange) and AD1-9 *cdc28-1* (purple) strains is shown. **C-** Quantification of Hxk levels normalized to loading in both AD1-9 (orange) and AD1-9 *cdc28-1* (purple) strains is shown). The values shown are the mean ±SEM (n=2).

4.7 Hit xanthones 5 and 17 decrease Cdc28 levels

Halo inhibition assays do not provide information regarding the element of the chaperone complex being targeted by the tested compounds. As mentioned above, Hsp90 inhibition can occur through 1) the binding to either NTD or CTD of Hsp90; 2) the disruption of the interaction between Hsp90 and co-chaperone; and 3) disruption of the interaction between the co-chaperone and the target proteins. However, the lack of inhibition induced by PPI inhibitors in the yeast models appear to indicate that the selected hit compounds may be targeting Hsp90 or Cdc37 binding to the target kinases. The destabilization of protein targets that rely on the Hsp90-Cdc37 chaperone complex such as Cdc28, without destabilizing Cdc37-independent target proteins levels, indicates a potential inhibition mechanism characteristic of Hsp90-Cdc37 specific inhibitors. In order to assess the potential destabilization of Cdc37-independent protein target Hxk and Cdc37-dependent protein target Cdc28, AD1-9 strain cells were grown in liquid cultures to log phase in the presence of xanthones 3, 5 and 17 (at 10 µg/mL), 6 (at 15 µg/mL), or 9 (at 5 µg/mL), or 17-AAG (indicator of Hsp90 inhibition at 1 µg/mL), or with the same volume of DMSO as control. The cells were collected and used to perform a western blot assay. All the compounds tested shown a tendency to induce the decrease of Cdc28 levels, which was more evident and statistically significant for xanthones 5 and 17 (**Fig. 13A** and **13B**). The strongest effect for these compounds is in agreement with the halo inhibition assays, since these were the compounds with the strong differential effect on growth inhibition. Surprisingly, xanthone 9 which caused the strongest inhibitory effect in liquid media, had almost no effect on Cdc28 levels. Since this compound exhibited some halo formation in the control AD1-9 strain, this result suggests that at least some growth inhibitory effects of xanthone 9 are Hsp90 independent. Concerning the levels of Hxk (**Fig. 13A** and **13C**), neither the compounds nor 17-AAG had any statistically significant effect.

Overall, these results showed that two of the hit xanthones, 5 and 17, appeared to decrease the Cdc37-dependent target Cdc28 but not the Cdc37-independent target Hxk. However, since even for the control 17-AAG the results for Hxk were not statistically significant, and the compounds exhibited a tendency to reduce Hxk levels, further replicates will be required to determine the inhibition mechanism induced by the selected xanthones.

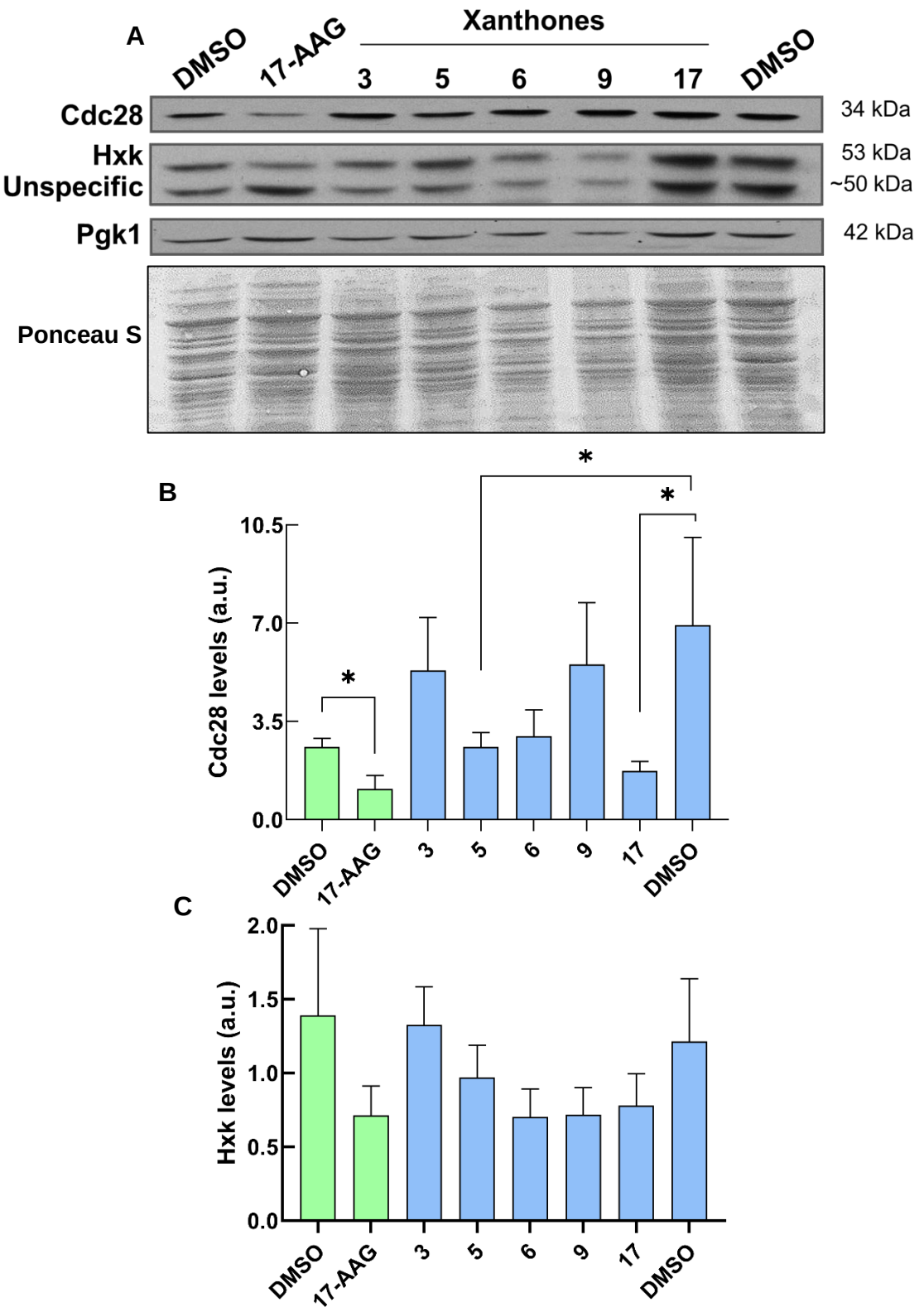

Figure 13- Screening compounds destabilize Cdc28 in AD1-9 strain. A- *S. cerevisiae* AD1-9 cells were grown to early exponential (log) phase in liquid YPD medium and treated with the solvent DMSO (negative control), Hsp90 inhibitor 17-AAG (1µg/mL) and xanthones 3, 5, 17 (10 µg/mL), 6 (15 µg/mL) and 9 (5 µg/mL). Cdc28 and Hxk levels were assessed by western blotting. Total protein staining with Ponceau S is also shown. The average between Pgk1 and indicated unspecific band was used as loading control. **B-** Quantification of Cdc28 levels normalized to loading is shown. **C-** Quantification of Hxk levels normalized to loading in both. Separate DMSO controls for 17-AAG (green) and xanthones (blue) activity were used. The values shown are the mean ±SEM with $p<0.05$ (n=4).

5. Conclusion and Future Perspectives

Hsp90 is a highly conserved and ubiquitously expressed molecular chaperone that occupies a central role in establishing interactions with over 400 client proteins (Farid Ahmad Siddiqui et al., 2021; Taipale et al., 2010) through the formation of chaperone complexes with over 20 co-chaperone proteins such as Cdc37 (Taipale et al., 2010). The development of Hsp90 inhibitors is highly relevant for therapeutical approaches, and several compounds have been identified. However, to this date no inhibitor has received clinical approval due to off-target effects (characteristic of Hsp90 NTD inhibitors) (Serwetnyk & Blagg, 2021). The development of Hsp90-Cdc37 or Cdc37-kinase PPI inhibitors may represent a more targeted approach and allow for the elimination of off-target effects.

The yeast represents an excellent model in the process of drug discovery due to its short life cycle, inexpensive growth and maintenance and easy genetic manipulation (Rezwan & Auerbach, 2012). To our knowledge, yeast-based models for the screening of inhibitors of the Hsp90-Cdc37 interaction have not been developed and the study of compounds targeting this interaction is achieved mainly through *in vitro* mammalian cell lysate-based assays (Serwetnyk & Blagg, 2021; Siddiqui et al., 2020). Regarding Hsp90, a yeast model expressing the human Hsp90 protein has been developed that could potentially be used to screen compounds with Hsp90 inhibitory activity (Piper et al., 2003). However, this model does not allow to distinguish Hsp90-Cdc37 PPI inhibition from Cdc37 inhibition. Alternatively, yeast two-hybrid (Y2H) assays can be employed to screen for disruptors of interactions between two proteins (Rezwan & Auerbach, 2012). A typical yeast two-hybrid assay is carried out by expressing one protein of interest fused with a DNA binding domain associated with a reporter gene and another one fused with a transactivation domain. The interaction of both proteins leads to the expression of an “hybrid” transcription factor that activates the reporter gene whose signal can be measured. However, this method is more expensive and time-consuming and does not allow to detect for Cdc37-kinase PPI inhibitors. While in theory it could be possible to construct a Y2H assay for Cdc37 interaction with a specific target kinase (e.g. Cdc28), it may not work because the interaction of Cdc37 with its kinase clients is transient, and the Y2H assay was designed to detect stable protein-protein interactions (Millson et al., 2004).

Yeast based approaches establish leading models regarding the screening of compounds in the early stages of drug discovery. In this work we aimed to develop a

yeast-based screening model for inhibitors of Hsp90, Hsp90-Cdc37 PPI and Cdc37-kinase PPI. Using a drug hypersensitive strain AD1-9 strain containing the *cdc28-1* mutation, we were able to establish a screening model that displayed enhanced sensitivity to known Hsp90 inhibitors but mostly retained the same sensitivity to broad inhibitors such as cycloheximide. The inhibition halo assays performed not only permitted the simultaneous analysis of multiple compounds in a single petri dish, but also provided the ability to easily assess the effect of multiple concentrations of all tested compound in a single assay. Through the size of the inhibition halo formed in the sensitive AD1-9 *cdc28-1* strain versus the AD1-9 strain, several promising compounds were selected for further analysis. Despite testing distinct classes of compounds, the hit compounds were all xanthones. Known surface PPI inhibitors of the interaction established between Hsp90 and Cdc37, platycodin D and elaiophylin, were employed in the yeast halo assay in order to determine how their effect would compare with the xanthones selected. Unfortunately, no growth inhibition was observed upon treatment of AD1-9 cells with these compounds. While the sequence identity shared between the yeast Hsp90 ortholog (Hsc82) and the cytosolic mammalian Hsp90 is approximately 60% (Verba & Agard, 2017), the sequence identity shared by Cdc37 orthologs is only about 19%. Therefore, our screening model lacked the ability to accurately mimic the different interactions that the tested compounds could establish with the human Cdc37 (p50). Hence, throughout the initial screening, compounds that could interact with the human Cdc37 protein but not with the yeast orthologue may have been disregarded, and the opposite, compounds that may inhibit yeast Hsp90-Cdc37 may not be functional in the human interaction. The lack of accuracy shown by the developed screening model is emphasized by the absence of visible growth arrest induced by known specific surface PPI inhibitors platycodin D and elaiophylin, capable of disrupting the interaction established between Hsp90 and human Cdc37. One of the major advantages associated with the yeast model is the simplicity associated with its genetic manipulation that allow for the expression of non-yeast proteins in yeast cells. In order to overcome the low identity shared between the yeast and human Cdc37 orthologues, we developed the AD1-9 *cdc37Δ* p50-*CDC37* strain expressing the chimeric human-yeast *CDC37* gene and the AD1-9 *cdc37Δ* O.E. p50 strain overexpressing the full-length human p50 gene. The chimeric *CDC37* gene possesses the human p50 NTD (responsible for client protein interaction) and therefore can improve upon the previous established screening model by accurately portraying the effect inhibitory compounds may cause in the interaction established between the Hsp90-Cdc37 chaperone complex and client proteins in human cells. However, the chimeric gene retains the yeast middle domain responsible for Hsp90

interaction. This represents a limitation that hinder the chimeric model's ability to identify specific Hsp90-Cdc37 interaction inhibitors. The complete replacement of the endogenous *CDC37* gene with the human p50 improves upon the developed chimeric model by potentially allowing for both the screening of inhibitors that target the interaction established by the chaperone complex with client proteins, in this case Cdc28, and the ones that target the interaction between Hsp90 and Cdc37 in human cells such as the known surface PPI inhibitors platycodin D and elaiophylin. However, the known PPI inhibitors tested remained unable to induce growth arrest in the newly developed models. These results lead us to infer that the lack of growth inhibition in the presence of Hsp90-Cdc37 interaction inhibitors did not stem only from the lack of homology between Cdc37 and p50. As such, we have put forward three hypotheses: i) despite sharing 60% sequence identity with yeast orthologues Hsc82 and Hsp82, Hsp90 may still possess crucial differences that alter the way it interacts with Cdc37. These differences may prevent our model to accurately depict the interaction between Hsp90 and Cdc37 targeted by the used PPI inhibitors. The development of a fully humanized yeast model expressing both p50 and Hsp90 human proteins would provide a more accurate target for inhibition. ii) the PPI inhibitors tested are novel compounds that may lack the reported efficiency and be unable to cause a significant disruption of Hsp90-Cdc37 interaction. The employment of other known inhibitors such as conglobatin and derrubone would provide further insight regarding this hypothesis. iii) The disruption of Hsp90-Cdc37 interaction may not cause growth arrest in yeast. It has been reported that, in the absence of Hsp90, Cdc37 is able to display independent chaperone activities supporting yeast growth and protein folding (MacLean & Picard, 2003) and therefore may be able to assure the proper folding of sufficient Cdc28 to ensure cell growth. In this case, the halo assays employed to detect compounds capable of inducing growth arrest would be unable to detect Hsp90-Cdc37 interaction inhibitors. A valid alternative would be the implementation of a reverse yeast two-hybrid assay. This system has been adapted so that the interaction between the proteins leads to the activation of a toxic reporter gene that leads to cell death when grown in a selective medium. The addition of compounds that would successfully inhibit the interaction between the proteins would prevent the activation of the toxic reporter gene and allow normal cell growth (Rezwan & Auerbach, 2012). This yeast two-hybrid system would provide a way to counteract Cdc37 potential independent activity and accurately identify Hsp90-Cdc37 interaction inhibitors while our halo assays would oversee the identification of inhibitors that target either Hsp90 or Cdc37. Moreover, if the growth arrest induced by the selected xanthones resulted from the ability to target either Hsp90 or Cdc37, previously tested compounds that, as the

known PPI inhibitors tested, have failed to produce an inhibition halo could be tested using the yeast two-hybrid assay to verify their potential as protein interaction inhibitors.

In order to determine how the selected hit xanthones were inhibiting cell growth, the level of proteins that rely on Hsp90, the Hsp90-Cdc37 chaperone complex or Cdc37 were assessed. The protein hexokinase was chosen to identify inhibitors targeting Hsp90 in a Cdc37-independent manner (Girstmair et al., 2019) and Cdc28 was selected as a protein that requires the proper Hsp90-Cdc37 chaperone complex activity, or at least a functional Cdc37 protein to acquire stability (Pearl & Prodromou, 2006). We postulated that the treatment of yeast cells with Hsp90 known inhibitor 17-AAG would induce the destabilization of both Cdc37-dependent and independent proteins (i.e., would lead to the reduction of both Hxk and Cdc28 levels), while the treatment with Hsp90-Cdc37 PPI inhibitors would only affect Cdc28 levels. We found that, like in mammalian cells, 17-AAG treatment leads to a decrease in Cdc28 levels in yeast, indicating it can be used as a marker for Hsp90-Cdc37 inhibition. However, the effect of 17-AAG on Hxk levels is more variable and although there was a tendency for Hxk to decrease upon 17-AAG treatment, the effect was not robust enough to be statistically significant and therefore it may not be a good marker for Hsp90-dependent Cdc37-independent target. Xanthone 9 had to be used at a lower concentration than the other xanthones (5 µg/mL instead of 10 µg/mL) because of the higher inhibition effect in the AD1-9 control strain using the halo assays. The inhibition of the control strain by xanthone 9 may be unrelated to the Hsp90-Cdc37 pathway as it did not cause Cdc28 destabilization. The remaining xanthones appeared to cause some Cdc28 destabilization, though only significant for xanthones 5 and 17. In accordance with what was verified with the inhibition halo assay, compounds 5 and 17 appear to be the xanthones responsible both for a more pronounced growth inhibition and a significant reduction of Cdc28 levels. Since Hsp90-Cdc37 inhibition leads to unfolding followed by degradation, some of the compounds may inhibit growth due to unfolding and loss of Cdc28 activity, but its effects in protein degradation may not be so easily detected. In this case, the halo assay would be more sensitive in the identification of potential inhibitors than the analysis of target destabilization by western blot assays. However, similar to 17-AAG treatment, some of the tested compounds appeared to lead to a slight decrease of Cdc37-independent target Hxk, however, this reduction was not statistically significant to allow conclusions to be drawn. The identification of a novel Cdc37-independent Hsp90 target that can be used as a reliable marker will be important for future works as well as the employment of a specific Hsp90-Cdc37 PPI inhibitor to confirm that this marker is Cdc37-inhibition independent. To identify the xanthones mechanism of action, molecular docking can be applied to map a prediction of the

interactions between the hit xanthones selected and Hsp90/Cdc37 at an atomic level, identifying possible Hsp90 /Cdc37 binding sites as well as characterizing the xanthone behaviour (conformation, position, and orientation) (Meng et al., 2011). Furthermore, binding of potential inhibitors of Hsp90 or Cdc37 can be confirmed through surface plasmon resonance (SPR). This is an optical technique where a ligand (Hsp90 or Cdc37) is immobilized on a metal surface containing a sensor while the different compounds are injected in a continuous flow across the surface. The binding of compounds to Hsp90 or Cdc37 leads to an increase in the surface refractive index in real time, characterizing the interaction (binding affinity and kinetics) (Patching, 2014).

In conclusion, we implemented a yeast model for the screening of inhibitors of the Hsp90-Cdc37 pathway and identified two promising xanthones inhibitors. Future work will be needed to improve this model toward the identification of Hsp90-Cdc37 PPI inhibitors. Also, it will be important to identify hit xanthones as Hsp90-Cdc37 or Cdc37-kinase PPI inhibitors or as general Hsp90 inhibitors like 17-AAG.

Given the lack of clinically approved Hsp90 inhibitors (due to high toxicity or loss of loss of activity in vivo) the identification of novel inhibitors of this pathway may be a valuable discovery. Natural xanthones are a large group of compounds found mostly in higher plants, displaying numerous biological activities (e.g., antimicrobial, anticancer, cardioprotective, antioxidant, immunoregulatory) (Singh et al., 2016). Natural xanthones possess a large structure variety according to the nature of substituents present, and tools have been developed that can easily introduce additional modifications to their structure in order to improve their natural biological activity, highlighting the potential of xanthone derivatives in the development of efficient drugs. To date, no Hsp90-Cdc37 inhibitor has not been discovered belonging to the class of xanthones, therefore, this class, comprised of oxygenated heterocycles, may represent a novel group of Hsp90 inhibitors (Pinto et al., 2005). Despite the weaker inhibitory effect displayed by the selected xanthones in comparison to 17-AAG, they represent a promissory alternative to be used as lead compounds upon which further manipulations can be implemented in order to develop derivatives with enhanced activity/potency and low side-effects.

6. References

Bandhakavi, S., McCann, R. O., Hanna, D. E., & Glover, C. V. (2003). A positive feedback loop between protein kinase CKII and Cdc37 promotes the activity of multiple protein kinases. *J Biol Chem*, *278*(5), 2829-2836.

Banerji, U., O'Donnell, A., Scurr, M., Pacey, S., Stapleton, S., Asad, Y., Simmons, L., Maloney, A., Raynaud, F., Campbell, M., Walton, M., Lakhani, S., Kaye, S., Workman, P., & Judson, I. (2005). Phase I pharmacokinetic and pharmacodynamic study of 17-allylamino, 17-demethoxygeldanamycin in patients with advanced malignancies. *J Clin Oncol*, *23*(18), 4152-4161.

Bascos, N. A. D., & Landry, S. J. (2019). A History of Molecular Chaperone Structures in the Protein Data Bank. *Int J Mol Sci*, *20*(24).

Biebl, M. M., Riedl, M., & Buchner, J. (2020). Hsp90 Co-chaperones Form Plastic Genetic Networks Adapted to Client Maturation. *Cell rep*, *32*(8), 108063.

Buolamwini, J., & Adjei, A. (2003). Novel Anticancer Drug Protocols. *85*.

Cadek, R., Chládková, K., Sigler, K., & Gásková, D. (2004). Impact of the growth phase on the activity of multidrug resistance pumps and membrane potential of *S. cerevisiae*: effect of pump overproduction and carbon source. *BBA*, *1665*(1-2), 111-117.

Castro-Alvarez, J. F., Uribe-Arias, A., & Cardona-Gómez, G. P. (2015). Cyclin-Dependent kinase 5 targeting prevents β-Amyloid aggregation involving glycogen synthase kinase 3β and phosphatases. *J Neurosci Res*, *93*(8), 1258-1266.

Chakraborty, A., & Edkins, A. L. (2020). Hop depletion reduces HSF1 levels and activity and coincides with reduced stress resilience. *Biochem. Biophys. Res. Commun.*, *527*(2), 440-446.

Clevenger, R. C., & Blagg, B. S. (2004). Design, synthesis, and evaluation of a radicicol and geldanamycin chimera, radamide. *Org Lett*, *6*(24), 4459-4462.

Cunningham, C. N., Krukenberg, K. A., & Agard, D. A. (2008). Intra- and intermonomer interactions are required to synergistically facilitate ATP hydrolysis in Hsp90. *J Biol Chem*, *283*(30), 21170-21178.

Czemeres, J., Buse, K., & Verkhivker, G. M. (2017). Atomistic simulations and network-based modeling of the Hsp90-Cdc37 chaperone binding with Cdk4 client protein: A mechanism of chaperoning kinase clients by exploiting weak spots of intrinsically dynamic kinase domains. *PLoS One*, *12*(12), e0190267.

Daniel Gietz, R., & Woods, R. A. (2002). Transformation of yeast by lithium acetate/single-stranded carrier DNA/polyethylene glycol method. In C. Guthrie & G. R. Fink (Eds.), *Methods in Enzymology* (Vol. 350, pp. 87-96). *AP*.

Devaney, E., & Gillan, V. (2016). Hsp90 Inhibitors in Parasitic Nematodes: Prospects and Challenges. *Curr Top Med Chem*, *16*(25), 2805-2811.

Dill, K. A., & MacCallum, J. L. (2012). The Protein-Folding Problem, 50 Years On. *Science*, *338*(6110), 1042-1046.

Donnelly, A., & Blagg, B. S. (2008). Novobiocin and additional inhibitors of the Hsp90 C-terminal nucleotide-binding pocket. *Curr Med Chem*, *15*(26), 2702-2717.

Dunker, A. K., Silman, I., Uversky, V. N., & Sussman, J. L. (2008). Function and structure of inherently disordered proteins. *Curr Opin Struct Biol*, *18*(6), 756-764.

Eccles, S. A., Massey, A., Raynaud, F. I., Sharp, S. Y., Box, G., Valenti, M., Patterson, L., de Haven Brandon, A., Gowan, S., Boxall, F., Aherne, W., Rowlands, M., Hayes, A., Martins, V., Urban, F., Boxall, K., Prodromou, C., Pearl, L., James, K., . . . Workman, P. (2008). NVP-AUY922: a novel heat shock protein 90 inhibitor active against xenograft tumor growth, angiogenesis, and metastasis. *Cancer Res*, *68*(8), 2850-2860.

Ellis, R. J. (2007). Protein misassembly: macromolecular crowding and molecular chaperones. *Adv Exp Med Biol*, *594*, 1-13.

Fadden, P., Huang, K. H., Veal, J. M., Steed, P. M., Barabasz, A. F., Foley, B., Hu, M., Partridge, J. M., Rice, J., Scott, A., Dubois, L. G., Freed, T. A., Silinski, M. A., Barta, T. E., Hughes, P. F., Ommen, A., Ma, W., Smith, E. D., Spangenberg, A. W., . . . Hall, S. E. (2010). Application of chemoproteomics to drug discovery: identification of a clinical candidate targeting hsp90. *Chem Biol*, *17*(7), 686-694.

Farrell, A., & Morgan, D. O. (2000). Cdc37 promotes the stability of protein kinases Cdc28 and Cak1. *Mol Cell Biol*, *20*(3), 749-754.

Fuhrmann-Stroissnigg, H., Ling, Y. Y., Zhao, J., McGowan, S. J., Zhu, Y., Brooks, R. W., Grassi, D., Gregg, S. Q., Stripay, J. L., Dorronsoro, A., Corbo, L., Tang, P., Bukata, C., Ring, N., Giacca, M., Li, X., Tchkonia, T., Kirkland, J. L., Niedernhofer, L. J., & Robbins, P. D. (2017). Identification of HSP90 inhibitors as a novel class of senolytics. *Nat. Commun.*, *8*(1), 422.

Funakoshi, M., & Hochstrasser, M. (2009). Small epitope-linker modules for PCR-based C-terminal tagging in *Saccharomyces cerevisiae*. *Yeast*, *26*(3), 185-192.

Ge, J., Normant, E., Porter, J. R., Ali, J. A., Dembski, M. S., Gao, Y., Georges, A. T., Grenier, L., Pak, R. H., Patterson, J., Sydor, J. R., Tibbitts, T. T., Tong, J. K., Adams, J., & Palombella, V. J. (2006). Design, synthesis, and biological evaluation of hydroquinone derivatives of 17-amino-17-demethoxygeldanamycin as potent, water-soluble inhibitors of Hsp90. *J Med Chem*, *49*(15), 4606-4615.

Girstmair, H., Tippel, F., Lopez, A., Tych, K., Stein, F., Haberkant, P., Schmid, P. W. N., Helm, D., Rief, M., Sattler, M., & Buchner, J. (2019). The Hsp90 isoforms from *S. cerevisiae* differ in structure, function and client range. *Nat. Commun.*, *10*(1), 3626.

Gracia, L., Lora, G., Blair, L. J., & Jinwal, U. K. (2019). Therapeutic Potential of the Hsp90/Cdc37 Interaction in Neurodegenerative Diseases [Mini Review]. *Front. Neurosci.*, *13*.

Gui, M., Zhang, M. X., Wu, W. H., & Sun, P. (2019). Natural Occurrence, Bioactivity and Biosynthesis of Elaiophylin Analogues. *Molecules*, *24*(21).

Hadden, M. K., Galam, L., Gestwicki, J. E., Matts, R. L., & Blagg, B. S. (2007). Derrubone, an inhibitor of the Hsp90 protein folding machinery. *J Nat Prod*, *70*(12), 2014-2018.

Hainzl, O., Lapina, M. C., Buchner, J., & Richter, K. (2009). The charged linker region is an important regulator of Hsp90 function. *J Biol Chem*, *284*(34), 22559-22567.

Hanahan, D., & Weinberg, R. A. (2000). The hallmarks of cancer. *Cell*, *100*(1), 57-70.

Hartl, F. U., Bracher, A., & Hayer-Hartl, M. (2011). Molecular chaperones in protein folding and proteostasis. *Nature*, *475*(7356), 324-332.

Hartl, F. U., & Hayer-Hartl, M. (2009). Converging concepts of protein folding in vitro and in vivo. *Nat Struct Mol Biol*, *16*(6), 574-581.

Hawle, P., Horst, D., Bebelman, J. P., Yang, X. X., Siderius, M., & van der Vies, S. M. (2007). Cdc37p is required for stress-induced high-osmolarity glycerol and protein kinase C mitogen-activated protein kinase pathway functionality by interaction with Hog1p and Slt2p (Mpk1p). *Eukaryot. Cell*, *6*(3), 521-532.

Hong, D. S., Banerji, U., Tavana, B., George, G. C., Aaron, J., & Kurzrock, R. (2013). Targeting the molecular chaperone heat shock protein 90 (HSP90): lessons learned and future directions. *Cancer Treat Rev*, *39*(4), 375-387.

Hoter, A., El-Sabban, M. E., & Naim, H. Y. (2018). The HSP90 Family: Structure, Regulation, Function, and Implications in Health and Disease. *Int J Mol Sci*, *19*(9).

Huang, W., Ye, M., Zhang, L. R., Wu, Q. D., Zhang, M., Xu, J. H., & Zheng, W. (2014). FW-04-806 inhibits proliferation and induces apoptosis in human breast cancer cells by binding to N-terminus of Hsp90 and disrupting Hsp90-Cdc37 complex formation. *Mol Cancer*, *13*, 150.

Hughes, T. R. (2002). Yeast and drug discovery. *Funct Integr Genomics*, *2*(4-5), 199-211.

Jackson, S. E. (2013). Hsp90: structure and function. *Top Curr Chem*, *328*, 155-240.

Jinwal, U. K., Trotter, J. H., Abisambra, J. F., Koren, J., 3rd, Lawson, L. Y., Vestal, G. D., O'Leary, J. C., 3rd, Johnson, A. G., Jin, Y., Jones, J. R., Li, Q., Weeber, E. J., & Dickey, C. A. (2011). The Hsp90 kinase co-chaperone Cdc37 regulates tau stability and phosphorylation dynamics. *J Biol Chem*, *286*(19), 16976-16983.

Johnson, J. L. (2012). Evolution and function of diverse Hsp90 homologs and cochaperone proteins. *Biochim Biophys Acta*, *1823*(3), 607-613.

Keramisanou, D., Aboalroub, A., Zhang, Z., Liu, W., Marshall, D., Diviney, A., Larsen, R. W., Landgraf, R., & Gelis, I. (2016). Molecular Mechanism of Protein Kinase Recognition and Sorting by the Hsp90 Kinome-Specific Cochaperone Cdc37. *Mol Cell*, *62*(2), 260-271.

Khandelwal, A., Crowley, V. M., & Blagg, B. S. J. (2016). Natural Product Inspired N-Terminal Hsp90 Inhibitors: From Bench to Bedside? *Med Res Rev*, *36*(1), 92-118.

Kitazono, A. A., Garza, D. A., & Kron, S. J. (2003). Mutations in the yeast cyclin-dependent kinase Cdc28 reveal a role in the spindle assembly checkpoint. *Mol Genet Genomics*, *269*(5), 672-684.

Lamoth, F., Juvvadi, P. R., & Steinbach, W. J. (2016). Heat shock protein 90 (Hsp90): A novel antifungal target against Aspergillus fumigatus. *Crit Rev Microbiol*, *42*(2), 310-321.

Li, J., & Buchner, J. (2013). Structure, function and regulation of the hsp90 machinery. *Biomed J*, *36*(3), 106-117.

Li, S., Li, J., Hu, T., Zhang, C., Lv, X., He, S., Yan, H., Tan, Y., Wen, M., Lei, M., & Zuo, J. (2017). Bcl-2 overexpression contributes to laryngeal carcinoma cell survival by forming a complex with Hsp90β. *Oncol Rep*, *37*(2), 849-856.

Li, T., Chen, X., Dai, X. Y., Wei, B., Weng, Q. J., Chen, X., Ouyang, D. F., Yan, R., Huang, Z. J., Jiang, H. L., Zhu, H., & Lu, J. J. (2017). Novel Hsp90 inhibitor platycodin D disrupts Hsp90/Cdc37 complex and enhances the anticancer effect of mTOR inhibitor. *Toxicol Appl Pharmacol*, *330*, 65-73.

Li, T., Jiang, H.-L., Tong, Y.-G., & Lu, J.-J. (2018). Targeting the Hsp90-Cdc37-client protein interaction to disrupt Hsp90 chaperone machinery. *J. Hematol. Oncol.*, *11*(1), 59.

Li, Y., Zhang, D., Xu, J., Shi, J., Jiang, L., Yao, N., & Ye, W. (2012). Discovery and development of natural heat shock protein 90 inhibitors in cancer treatment. *Acta Pharm. Sin. B.*, *2*(3), 238-245.

Lian, J., Lin, D., Xie, X., Xu, Y., Xu, L., Meng, L., & Zhu, Y. (2017). NVP-AUY922, a novel HSP90 inhibitor, inhibits the progression of malignant pheochromocytoma in vitro and in vivo. *Onco Targets Ther*, *10*, 2219-2226.

Liu, C., Apodaca, J., Davis, L. E., & Rao, H. (2007). Proteasome inhibition in wild-type yeast *Saccharomyces cerevisiae* cells. *BioTechniques*, *42*(2), 158-162.

Ma, M., & Liu, Z. L. (2010). Comparative transcriptome profiling analyses during the lag phase uncover YAP1, PDR1, PDR3, RPN4, and HSF1 as key regulatory genes in genomic adaptation to the lignocellulose derived inhibitor HMF for *Saccharomyces cerevisiae*. *BMC Genomics*, *11*, 660.

MacLean, M., & Picard, D. (2003). Cdc37 goes beyond Hsp90 and kinases. *Cell Stress Chaperones*, *8*(2), 114-119.

McClellan, A. J., Tam, S., Kaganovich, D., & Frydman, J. (2005). Protein quality control: chaperones culling corrupt conformations. *Nat. Cell Biol.*, *7*(8), 736-741.

Meng, X. Y., Zhang, H. X., Mezei, M., & Cui, M. (2011). Molecular docking: a powerful approach for structure-based drug discovery. *Curr Comput Aided Drug Des*, *7*(2), 146-157.

Millson, S. H., Prodromou, C., & Piper, P. W. (2010). A simple yeast-based system for analyzing inhibitor resistance in the human cancer drug targets Hsp90alpha/beta. *Biochem Pharmacol*, *79*(11), 1581-1588.

Millson, S. H., Truman, A. W., Wolfram, F., King, V., Panaretou, B., Prodromou, C., Pearl, L. H., & Piper, P. W. (2004). Investigating the protein-protein interactions of the yeast Hsp90 chaperone system by two-hybrid analysis: potential uses and limitations of this approach. *Cell Stress Chaperones*, *9*(4), 359-368.

Mollapour, M., Tsutsumi, S., Truman, A. W., Xu, W., Vaughan, C. K., Beebe, K., Konstantinova, A., Vourganti, S., Panaretou, B., Piper, P. W., Trepel, J. B., Prodromou, C., Pearl, L. H., & Neckers, L. (2011). Threonine 22 phosphorylation attenuates Hsp90 interaction with cochaperones and affects its chaperone activity. *Mol Cell*, *41*(6), 672-681.

Nawrocki, A., Fey, S. J., Goffeau, A., Roepstorff, P., & Larsen, P. M. (2001). The effects of transcription regulating genes PDR1, pdr1-3 and PDR3 in pleiotropic drug resistance. *Proteomics*, *1*(8), 1022-1032.

Patching, S. G. (2014). Surface plasmon resonance spectroscopy for characterisation of membrane protein-ligand interactions and its potential for drug discovery. *Biochim Biophys Acta*, *1838*(1 Pt A), 43-55.

Paumi, C. M., Chuk, M., Snider, J., Stagljar, I., & Michaelis, S. (2009). ABC transporters in *Saccharomyces cerevisiae* and their interactors: new technology advances the biology of the ABCC (MRP) subfamily. *Microbiol Mol Biol Rev*, *73*(4), 577-593.

Pearl, L. H. (2005). Hsp90 and Cdc37 -- a chaperone cancer conspiracy. *Curr Opin Genet Dev*, *15*(1), 55-61.

Pearl, L. H., & Prodromou, C. (2006). Structure and mechanism of the Hsp90 molecular chaperone machinery. *Annu Rev Biochem*, *75*, 271-294.

Peng, S., Woodruff, J., Pathak, P. K., Matts, R. L., & Deng, J. (2022). Crystal structure of the middle and C-terminal domains of Hsp90α labeled with a coumarin derivative reveals a potential allosteric binding site as a drug target. *Acta Crystallogr D Struct Biol*, *78*(Pt 5), 571-585.

Pinto, M. M., Sousa, M. E., & Nascimento, M. S. (2005). Xanthone derivatives: new insights in biological activities. *Curr Med Chem*, *12*(21), 2517-2538.

Piper, P. W., & Millson, S. H. (2011). Mechanisms of Resistance to Hsp90 Inhibitor Drugs: A Complex Mosaic Emerges. *Pharmaceuticals (Basel)*, *4*(11), 1400-1422.

Piper, P. W., Panaretou, B., Millson, S. H., Truman, A., Mollapour, M., Pearl, L. H., & Prodromou, C. (2003). Yeast is selectively hypersensitised to heat shock protein 90 (Hsp90)-targetting drugs with heterologous expression of the human Hsp90beta, a property that can be exploited in screens for new Hsp90 chaperone inhibitors. *Gene*, *302*(1-2), 165-170.

Prodromou, C. (2016). Mechanisms of Hsp90 regulation. *Biochem J*, *473*(16), 2439-2452.

Prodromou, C., & Bjorklund, D. M. (2022). Advances towards Understanding the Mechanism of Action of the Hsp90 Complex. *Biomolecules*, *12*(5), 600.

Reidy, M., Kumar, S., Anderson, D. E., & Masison, D. C. (2018). Dual Roles for Yeast Sti1/Hop in Regulating the Hsp90 Chaperone Cycle. *Genetics*, *209*(4), 1139-1154.

Rezwan, M., & Auerbach, D. (2012). Yeast "N"-hybrid systems for protein-protein and drug-protein interaction discovery. *Methods*, *57*(4), 423-429.

Rogers, B., Decottignies, A., Kolaczkowski, M., Carvajal, E., Balzi, E., & Goffeau, A. (2001). The pleitropic drug ABC transporters from S*accharomyces cerevisiae*. *J Mol Microbiol Biotechnol*, *3*(2), 207-214.

Sahasrabudhe, P., Rohrberg, J., Biebl, M. M., Rutz, D. A., & Buchner, J. (2017). The Plasticity of the Hsp90 Co-chaperone System. *Mol Cell*, *67*(6), 947-961.e945.

Sequist, L. V., Gettinger, S., Senzer, N. N., Martins, R. G., Jänne, P. A., Lilenbaum, R., Gray, J. E., Iafrate, A. J., Katayama, R., Hafeez, N., Sweeney, J., Walker, J. R., Fritz, C., Ross, R. W., Grayzel, D., Engelman, J. A., Borger, D. R., Paez, G., & Natale, R. (2010). Activity of IPI-504, a novel heat-shock protein 90 inhibitor, in patients with molecularly defined non-small-cell lung cancer. *J Clin Oncol*, *28*(33), 4953-4960.

Serwetnyk, M. A., & Blagg, B. S. J. (2021). The disruption of protein-protein interactions with co-chaperones and client substrates as a strategy towards Hsp90 inhibition. *Acta Pharm Sin B*, *11*(6), 1446-1468.

Siddiqui, F. A., Parkkola, H., Manoharan, G. B., & Abankwa, D. (2020). Medium-Throughput Detection of Hsp90/Cdc37 Protein-Protein Interaction Inhibitors Using a Split Renilla Luciferase-Based Assay. *SLAS Discov*, *25*(2), 195-206.

Siddiqui, F. A., Parkkola, H., Vukic, V., Oetken-Lindholm, C., Jaiswal, A., Kiriazis, A., Pavic, K., Aittokallio, T., Salminen, T. A., & Abankwa, D. (2021). Novel Small Molecule Hsp90/Cdc37 Interface Inhibitors Indirectly Target K-Ras-Signaling. *Cancers*, *13*(4), 927.

Siddiqui, F. A., Vukic, V., Salminen, T. A., & Abankwa, D. (2021). Elaiophylin Is a Potent Hsp90/Cdc37 Protein Interface Inhibitor with K-Ras Nanocluster Selectivity. *Biomolecules*, *11*(6).

Simon, J. A., & Bedalov, A. (2004). Yeast as a model system for anticancer drug discovery. *Nat. Rev. Cancer*, *4*(6), 481-487.

Singh, A., Kaur, N., Sharma, S., & Bedi, P. M. S. (2016). Recent progress in biologically active xanthones. *8*, 75-131.

Taipale, M., Jarosz, D. F., & Lindquist, S. (2010). HSP90 at the hub of protein homeostasis: emerging mechanistic insights. *Nat. Rev. Mol. Cell Biol.*, *11*(7), 515-528.

Taldone, T., & Chiosis, G. (2009). Purine-scaffold Hsp90 inhibitors. *Curr Top Med Chem*, *9*(15), 1436-1446.

Tariq, M., Nussbaumer, U., Chen, Y., Beisel, C., & Paro, R. (2009). Trithorax requires Hsp90 for maintenance of active chromatin at sites of gene expression. *Proc Natl Acad Sci U S A*, *106*(4), 1157-1162.

Taylor, S. S., Keshwani, M. M., Steichen, J. M., & Kornev, A. P. (2012). Evolution of the eukaryotic protein kinases as dynamic molecular switches. *Philos Trans R Soc Lond B Biol Sci*, *367*(1602), 2517-2528.

Trendowski, M. (2015). PU-H71: An improvement on nature's solutions to oncogenic Hsp90 addiction. *Pharmacol Res*, *99*, 202-216.

Trepel, J., Mollapour, M., Giaccone, G., & Neckers, L. (2010). Targeting the dynamic HSP90 complex in cancer. *Nat Rev Cancer*, *10*(8), 537-549.

Turnbull, E. L., Martin, I. V., & Fantes, P. A. (2005). Cdc37 maintains cellular viability in *Schizosaccharomyces pombe* independently of interactions with heat-shock protein 90. *Febs j*, *272*(16), 4129-4140.

Vartholomaiou, E., Madon-Simon, M., Hagmann, S., Mühlebach, G., Wurst, W., Floss, T., & Picard, D. (2017). Cytosolic Hsp90α and its mitochondrial isoform Trap1 are differentially required in a breast cancer model. *Oncotarget*, *8*(11), 17428-17442.

Verba, K. A., & Agard, D. A. (2017). How Hsp90 and Cdc37 Lubricate Kinase Molecular Switches. *Trends Biochem Sci*, *42*(10), 799-811.

Verba, K. A., Wang, R. Y., Arakawa, A., Liu, Y., Shirouzu, M., Yokoyama, S., & Agard, D. A. (2016). Atomic structure of Hsp90-Cdc37-Cdk4 reveals that Hsp90 traps and stabilizes an unfolded kinase. *Science*, *352*(6293), 1542-1547.

Wang, L., Bergkvist, L., Kumar, R., Winblad, B., & Pavlov, P. F. (2021). Targeting Chaperone/Co-Chaperone Interactions with Small Molecules: A Novel Approach to Tackle Neurodegenerative Diseases. *Cells*, *10*(10).

Wang, X., Venable, J., LaPointe, P., Hutt, D. M., Koulov, A. V., Coppinger, J., Gurkan, C., Kellner, W., Matteson, J., Plutner, H., Riordan, J. R., Kelly, J. W., Yates, J. R., 3rd, & Balch, W. E. (2006). Hsp90 cochaperone Aha1 downregulation rescues misfolding of CFTR in cystic fibrosis. *Cell*, *127*(4), 803-815.

Wang, Y., Jin, F., Wang, R., Li, F., Wu, Y., Kitazato, K., & Wang, Y. (2017). HSP90: a promising broad-spectrum antiviral drug target. *Arch Virol*, *162*(11), 3269-3282.

Wang, Y. T., & Lu, J. H. (2022). Chaperone-Mediated Autophagy in Neurodegenerative Diseases: Molecular Mechanisms and Pharmacological Opportunities. *Cells*, *11*(14).

Workman, P., Burrows, F., Neckers, L., & Rosen, N. (2007). Drugging the cancer chaperone HSP90: combinatorial therapeutic exploitation of oncogene addiction and tumor stress. *Ann N Y Acad Sci*, *1113*, 202-216.

Xiao, Y., & Liu, Y. (2020). Recent Advances in the Discovery of Novel HSP90 Inhibitors: An Update from 2014. *Curr Drug Targets*, *21*(3), 302-317.

Xu, W., Mollapour, M., Prodromou, C., Wang, S., Scroggins, B. T., Palchick, Z., Beebe, K., Siderius, M., Lee, M. J., Couvillon, A., Trepel, J. B., Miyata, Y., Matts, R., & Neckers, L. (2012). Dynamic tyrosine phosphorylation modulates cycling of the HSP90-P50(CDC37)-AHA1 chaperone machine. *Mol Cell*, *47*(3), 434-443.

Xu, W., Yuan, X., Xiang, Z., Mimnaugh, E., Marcu, M., & Neckers, L. (2005). Surface charge and hydrophobicity determine ErbB2 binding to the Hsp90 chaperone complex. *Nat. Struct. Mol. Biol.*, *12*(2), 120-126.

Yang, S., Pascual-Guiral, S., Ponce, R., Giménez-Llort, L., Baltrons, M. A., Arancio, O., Palacio, J. R., Clos, V. M., Yuste, V. J., & Bayascas, J. R. (2018). Reducing the Levels of Akt Activation by PDK1 Knock-in Mutation Protects Neuronal Cultures against Synthetic Amyloid-Beta Peptides [Original Research]. *Front. Aging Neurosci.*, *9*.

Yu, Y., Hamza, A., Zhang, T., Gu, M., Zou, P., Newman, B., Li, Y., Gunatilaka, A. A., Zhan, C. G., & Sun, D. (2010). Withaferin A targets heat shock protein 90 in pancreatic cancer cells. *Biochem Pharmacol*, *79*(4), 542-551.

Zhang, J., Li, H., Liu, Y., Zhao, K., Wei, S., Sugarman, E. T., Liu, L., & Zhang, G. (2022). Targeting HSP90 as a Novel Therapy for Cancer: Mechanistic Insights and Translational Relevance. *Cells*, *11*(18).

Zhang, J., Yang, P. L., & Gray, N. S. (2009). Targeting cancer with small molecule kinase inhibitors. *Nat. Rev. Cancer*, *9*(1), 28-39.

Zhao, R., Davey, M., Hsu, Y. C., Kaplanek, P., Tong, A., Parsons, A. B., Krogan, N., Cagney, G., Mai, D., Greenblatt, J., Boone, C., Emili, A., & Houry, W. A. (2005). Navigating the chaperone network: an integrative map of physical and genetic interactions mediated by the hsp90 chaperone. *Cell*, *120*(5), 715-727.